Journal of Computational Physics 228 (2009) 8958–8984

Contents lists available at ScienceDirect

Journal of Computational Physics

journal homepage: www.elsevier.com/locate/jcp

The spectral order of accuracy: A new unified tool in the design methodology of excitation-adaptive wave equation FDTD schemes

B. Finkelstein, R. Kastner *

School of Electrical Engineering, Tel-Aviv University, Tel-Aviv 69978, Israel

ARTICLE INFO

Article history:
Received 15 January 2009
Received in revised form 30 August 2009
Accepted 31 August 2009
Available online 11 September 2009

Keywords:
Finite difference time domain
Numerical dispersion
Wave equation
Maxwell's equations
Nonstandard FDTD
Dispersion relation preserving schemes
Higher order schemes

ABSTRACT

We define a new concept, termed the spectral order of accuracy (SOoA), which is the spectral domain analogue of the familiar order of accuracy (OoA). The SOoA is pivotal in a refined version of a recently-introduced methodology for formulating excitation-adaptive wave equation FDTD (WE-FDTD) schemes, described below. This concept is the basis for a unified classification for both existing and new schemes. Both one- and two-dimensional cases are presented for boundless, source free, homogeneous, isotropic and lossless media. The 1-D and 2-D cases are developed in detail for the $(3,2M+1)$ (temporal, spatial) and $(3,3)$ 2-D stencils, respectively. Stability analysis is built into the methodology in terms of either analytical conditions or "stability maps" defined herein. The methodology is seen as a generalization of many existing schemes that also provides a unified tool for a systematical design of WE-FDTD schemes subject to specific requirements in terms of the spectral content of the excitation. The computational efficiency for all schemes remains the same for a given stencil, since the core of the FDTD code is unchanged between schemes, the difference being only in the values of scheme coefficients.

1. Introduction

An inherent error source in the finite difference time domain (FDTD) method [1,2] is the existence of numerical dispersion manifested by a numerical non-linear relationship $\tilde{k}(\omega)$. Remedies to dispersion errors were originally suggested in the form of dispersion relation preserving (DRP) schemes, introduced in [3] and continued in [4]. Other error reducing methods have included finer sampling rates, higher order schemes [5–13], and non-standard FDTD (NSFDTD) schemes [14–19]. Comparison between multiresolution and higher order for dispersion reduction schemes are presented in [20]. Minimization and optimization of predefined scheme properties (e.g. broadband dispersion error, anisotropy) methods have been developed, e.g. in [21–40].

A comprehensive methodology for the formulation of wave equation FDTD (WE-FDTD) schemes with controlled order of accuracy and dispersion has been recently introduced in [38–40]. The methodology is refined in this work by fusing both the order of accuracy (OoA) and numerical dispersion into the single concept of the spectral order of accuracy (SOoA). The SOoA is defined in the context of the general dispersion equation (GDE), i.e. the spectral transform of the discretized wave with undetermined coefficients [38,39]. In the process of reducing errors, one tries to fit the GDE to the linear dispersion surface, or, in the one-dimensional case, to the curve $K=\Omega/\gamma$, where $\Omega=\omega\Delta t$ and $K=\tilde{k}\Delta x$ and $\tilde{k}$ is the numerical wavenumber. Such a fit can be realized at the origin $(\Omega,K)=(0,0)$, in which case it is seen as an optimization of the OoA only. For a one-dimensional stencil with three temporal and $2M+1$ spatial samples (denoted herein as a $(3,2M+1)$ stencil), all schemes with OoAs

* Corresponding author. Tel.: +972 3 6407447; fax: +972 3 6423508.
E-mail address: kast@eng.tau.ac.il (R. Kastner).

0021-9991/$ - see front matter © 2009 Elsevier Inc. All rights reserved.
doi:10.1016/j.jcp.2009.08.034

ranging from $(2,2M)$ to $(2M,2M)$ are derived from a Taylor expansion of the GDE about the origin. However, the spectral domain representation makes it possible to fit the curves or surfaces at other frequency points to a certain order, denoted the SoOA. This general definition of the SOoA enables the optimization of the schemes about any range of finite frequencies Ω_q. The conventional OoA can then be traded for higher accuracy in terms of the phase or group velocities or higher order derivatives $\left(\left(\frac{\partial^n \tilde{k}}{\partial \omega^n}\right)^{-1}\right)$ at Ω_q. Note that the conventional OoA is directly related to the special case of the SOoA, defined about the origin of the dispersion surface. Using the SOoA, it becomes possible to design schemes tailored to a given excitation spectrum in order to reduce the overall error. Note also, that while the OoA determines the rate by which the difference equation converges to the PDE when $\Delta t \Rightarrow 0$ and $\Delta x, y \Rightarrow 0$, for a general Ω_q convergence is achieved (e.g. for the one-dimensional case) when $\Delta t \to \Delta t_q, \Delta x \to \Delta x_q \Rightarrow \Omega \to \Omega_q = \omega_q \Delta t_q, K \to K_q = \tilde{k}_q \Delta x_q$.

The process of fitting the GDE to the linear dispersion relationship begins with the selection of a set of frequencies in accordance with the spectral content of the exciting pulse and determination of the corresponding orders of accuracy by which the GDE converges to the linear curve about these frequencies. These choices are then translated into adjustments of certain coefficients within the scheme, as detailed in Section 2. The main FDTD code that follows this computation remains unchanged for all schemes pertaining to the given stencil.

Several cases are studied in Section 3. The methodology is applied to 1-D, source free homogeneous, isotropic, lossless and boundless wave equations, using stencils sizes of (3,3), (3,5) and (3,7) for explicit, central difference discretizations of the wave equation. The entire process is carried out while assuring numerical stability by the use of the general amplification polynomial (GAP).

An example of a wideband modulated pulse, propagated over a million time steps, with a (3,5) stencil is shown in Section 4, in comparison with the standard (4,4) scheme that uses the same stencil size and hence has the same computational complexity. The notable differences are in the group delay and distortions due to numerical dispersion. The two-dimensional case is initially developed in Section 5 with a suggestion for stencil classification and detailed development for the (3,3) stencil. This methodology can be seen as a generalization of available 1-D and 2-D schemes, that also provides a tool for devising new schemes tailored to the spectrum of the excitation. As seen in the examples, this process enables FDTD simulation over long periods of time with little dispersion error effects. The computational burden remains the same for all schemes because they only differ in the pre-calculations stage of the undetermined coefficients. Conclusions to this effect are drawn in Section 7.

2. Generation of one-dimensional schemes with specified spectral order of accuracy

2.1. Convergence rate of the wave equation in the spectral domain: the spectral order of accuracy (SOoA)

The equation to be discretized is the one-dimensional wave equation (WE) in a homogeneous, lossless, boundless and source free medium:

$$\left(\frac{\partial^2}{\partial t^2} - c^2 \frac{\partial^2}{\partial x^2}\right) E(x,t) = 0. \tag{1}$$

The conventional usage of a (3,3) stencil with the three point approximation of the second order derivatives in time and space leads to the following approximation of (1):

$$E_i^{n+1} - 2E_i^n + E_i^{n-1} - \gamma^2 \left(E_{i+1}^n - 2E_i^n + E_{i-1}^n\right) = 0, \quad \gamma = c\Delta t/\Delta x. \tag{2}$$

Eq. (2) can be generalized for temporal–spatial $(3,2M+1)$ stencils with symmetrical "molecules", typical of central differences:

$$\underbrace{E_i^{n+1} + E_i^{n-1}}_{\text{molecule}} + \sum_{m=0}^{M} c_m \underbrace{\left(E_{i+m}^n + E_{i-m}^n\right)}_{\text{molecule}} = 0. \tag{3}$$

Here, the molecule coefficients c_m serve as degrees of freedom for formulating many schemes. The number of these degrees of freedom is seen to be $M+1$ as determined by the stencil size. Upon invoking discrete separation of variables (or using the $\mathcal{Z}$-transform) in (3), i.e.

$$E_i^n = \xi^i(\Delta x)\tau^n(\Delta t) \tag{4}$$

and using the spectral representation $(\xi, \tau) = (e^{jK}, e^{j\,\Omega})$ where $\Omega = \omega\Delta t, K = \tilde{k}\Delta x$ ($\tilde{k}$ being the numerical wave number), the *generalized dispersion equation* (GDE) emerges

$$\cos\Omega + \sum_{m=0}^{M} c_m \cos mK = 0, \tag{5}$$

whose $\cos(\cdot)$ format is again typical of central differences. Eq. (5) is also the spatial–temporal spectral transform of (3). It is our objective to generate a scheme whose GDE curve (5) approximates the linear curve

$$-\Omega + \gamma K = 0 \tag{6}$$

subject to given requirements. The rate by which (5) converges to (6) is defined as the new concept of the spectral order of accuracy SOoA $= (N, I)$, where N and I characterize the convergence rates in Ω and K, respectively, as defined in Sections 2.2 and 2.3. One can define the SOoA about any arbitrary points (Ω_q, K_q) residing on the linear curve (6), including, but not limited to the case $(\Omega_q, K_q) = (0,0)$. The SOoA is defined per such point and is indexed accordingly as SOoA_q. The higher the SOoA, the higher the order of the GDE derivatives that are matched to the linear ones. For example, SOoA $= (1,1)$ at $(\Omega_q, K_q) > (0,0)$ is equivalent to matching the GDE curve with the linear curve by zero-order derivative only. In physical terms, this translates to the numerical phase velocity V_p matching the linear one at (Ω_q, K_q). Similarly, SOoA $= (2,2)$ is equivalent to matching both the GDE and its first derivative to those of the linear curve, or matching of both V_p and the group velocity V_g at (Ω_q, K_q) (for $(\Omega_q, K_q) = (0,0)$, matching of V_p only and of both V_p and V_g are characterized by SOoA $= (2,2)$ and $(4,4)$, respectively).

The conventional temporal/spatial OoA concept can be seen as a special case of the SOoA for $(\Omega_q, K_q) = (0,0)$, because the limits $\Delta x \to 0,\ \Delta t \to 0$ are synonymous with $\Omega \to 0,\ K \to 0$ (actually, the relationship is SOoA $=$ OoA $+ 2$).

In summary, the spectral domain methodology offers the benefit of unifying the standard and non-standard FDTD schemes while consolidating the parameters of the conventional OoA and dispersion reduction techniques under the single concept of the SOoA. In doing so, the framework for designing additional, tailor made schemes is revealed. Such schemes can be made to accommodate the spectra of specific excitations, for both narrowband and wideband signals.

2.2. The case $(\Omega_q, K_q) = (0,0)$

We wish to use (5) as an approximation to the linear dispersion relationship (6) about $(\Omega_q, K_q) = (0,0)$. To this end, expand (5) as a two-dimensional Taylor series about (0,0), equating the series to zero term by term up to the SOoA $= (N, I)$, as follows:

$$\sum_{p=0}^{\infty} \frac{(-1)^p}{(2p)!}\Omega^{2p} + \sum_{m=0}^{M} c_m \sum_{p=0}^{\infty} \frac{(-1)^p}{(2p)!}(mK)^{2p} = \sum_{p=0}^{\frac{N}{2}-1} \frac{(-1)^p}{(2p)!}\Omega^{2p} + \mathcal{O}(\Omega^N) + c_0 + \sum_{p=0}^{\frac{I}{2}-1}\sum_{m=1}^{M} c_m m^{2p} \frac{(-1)^p}{(2p)!}K^{2p} + \mathcal{O}(K^I) = 0, \tag{7}$$

where N and I are even numbers. Eq. (7) is compacted by defining $\mathbf{c} = (c_1, c_2, \ldots, c_M)$ and $\mathbf{v}^s = (1^s\, 2^s\, \ldots, M^s)^T$:

$$c_0 + \sum_{p=0}^{\frac{N}{2}-1} \frac{(-1)^p}{(2p)!}\Theta^{2p}(\Omega, K) + \sum_{p=\frac{N}{2}}^{\frac{I}{2}-1} \frac{(-1)^p}{(2p)!}(\mathbf{c}\cdot\mathbf{v}^{2p})K^{2p} + \mathcal{O}(\Omega^N + K^I) = 0, \tag{8}$$

where

$$\Theta^{2p}(\Omega, K) = \Omega^{2p} + (\mathbf{c}\cdot\mathbf{v}^{2p})K^{2p}. \tag{9}$$

Once the linear dispersion relationship (6) is substituted into the first summation in (8) and the series is truncated to $\mathcal{O}(\Omega^N + K^I)$ we have

$$c_0 + \sum_{p=0}^{\frac{N}{2}-1} \frac{(-1)^p}{(2p)!}\left[1 + \frac{(\mathbf{c}\cdot\mathbf{v}^{2p})}{\gamma^{2p}}\right]\Omega^{2p} + \sum_{p=\frac{N}{2}}^{\frac{I}{2}-1} \frac{(-1)^p}{(2p)!}(\mathbf{c}\cdot\mathbf{v}^{2p})K^{2p} = 0, \quad N \leqslant I \leqslant 2M+2. \tag{10}$$

Equating each of the terms in (10) to zero leads finally to a system of equations for determining the c_ms such that the truncated Taylor expansion of the GDE approximates the linear dispersion relationship to the specified SOoA:

$$1 + \sum_{m=0}^{M} c_m = 0, \quad p = 0, \tag{11a}$$

$$1 + \frac{(\mathbf{c}\cdot\mathbf{v}^{2p})}{\gamma^{2p}} = 0, \quad p = 1, \ldots, \frac{N}{2} - 1, \tag{11b}$$

$$\mathbf{c}\cdot\mathbf{v}^{2p} = 0, \quad p = \frac{N}{2}, \ldots, \frac{I}{2} - 1 \quad N \leqslant I \leqslant 2M+2. \tag{11c}$$

Eq. (11) serve as a design tool for new FDTD schemes given the $(3, 2M+1)$ stencil size. In designing these schemes, one has the freedom to choose the values of N and I almost arbitrarily. The choice of N determines the balance between equations of the type (11b) and (11c). The case of (11c) annuls the K-terms only, while Eq. (11b), that include the substitution of the linear dispersion relationship $K = \frac{\Omega}{\gamma}$ into the first summation in (8), annul both Ω and K-terms simultaneously. Eq. (11b) are the spectral domain equivalent of the temporal/spatial concept of "derivative swapping". For this reason, each addition of an equation of the type (11c) raises the value the order I only, whereas adding equations of the type (11b) raises the values of both N and I simultaneously. The parameters thus obey the condition $N \leqslant I \leqslant 2M+2$. The minimal $N_{\min} = 2$ is attained when only equations of the type (11c) are used, and the maximal $N_{\max} = I$ is where all the equation are of the type (11b).

If $I = I_{\max} = 2M+2$ and $N = I_{\max}$, then (10) is reduced to

$$c_0 + \sum_{p=0}^{M} \frac{(-1)^p}{(2p)!}\left[1 + \frac{(\mathbf{c}\cdot\mathbf{v}^{2p})}{\gamma^{2p}}\right]\Omega^{2p} = 0. \tag{12}$$

This special case coincides with Eq. (17) in [39]. Existing schemes, based on the conventional OoA, can be interpreted as certain choices of the value of N and I. For example, I can be set equal to $I_{\max} = 2M+2$, causing all degrees of freedom to be dedicated to the maximization of the OoA. Cases with $I < 2M+2$ allow tradeoffs where the OoA can be reduced in favor of non-Taylor based conditions, e.g. for dispersion error reduction at non-zero frequencies, sometimes referred to as non-standard schemes [32]. In the sequel, these methods, too, are consolidated into the more general framework based on the SOoA at a set of arbitrary frequencies.

2.3. The case $(\Omega_q, K_q) \neq (0,0)$

We begin the development by generalizing the definitions of Θ and $\mathbf{v}$ in (9) as follows:

$$\Theta^{2p}_{\cos}(\Omega_q, K_q) = \cos\Omega_q(\Omega-\Omega_q)^{2p} + \left(\mathbf{c}\cdot\mathbf{v}^{2p} * \mathbf{v}_{\cos}(K_q)\right)(K-K_q)^{2p}, \tag{13a}$$

$$\Theta^{2p+1}_{\sin}(\Omega_q, K_q) = \sin\Omega_q(\Omega-\Omega_q)^{2p+1} + \left(\mathbf{c}\cdot\mathbf{v}^{2p+1} * \mathbf{v}_{\sin}(K_q)\right)(K-K_q)^{2p+1}, \tag{13b}$$

$$\mathbf{v}_{\cos}(K_q) = (\cos K_q, \cos 2K_q, \ldots, \cos MK_q)^T, \tag{13c}$$

$$\mathbf{v}_{\sin}(K_q) = (\sin K_q, \sin 2K_q, \ldots, \sin MK_q)^T, \tag{13d}$$

where $\mathbf{c}$ and $\mathbf{v}^s$ have been defined above, $\mathbf{z} = \mathbf{x} * \mathbf{y} = (x_1y_1, x_2y_2, \ldots, x_My_M)$ and the * symbol denotes the Hadamard product. Incidentally, using these definitions, the GDE (5) may be re-stated as

$$c_0 + \cos\Theta_{\cos} - \sin\Theta_{\sin} = 0, \tag{14}$$

where

$$\cos\Theta_{\cos} = \sum_{p=0}^{\infty} \frac{(-1)^p}{(2p)!}\Theta^{2p}_{\cos}, \tag{15a}$$

$$\sin\Theta_{\sin} = \sum_{p=0}^{\infty} \frac{(-1)^p}{(2p+1)!}\Theta^{2p+1}_{\sin}. \tag{15b}$$

The generalized counterpart of (8) is obtained by expanding (5) about (Ω_q, K_q):

$$c_0 + \sum_{p=0}^{N-1}\eta_p\left(\alpha_p\Theta^p_{\cos} + (1-\alpha_p)\Theta^p_{\sin}\right) + \sum_{p=N}^{I-1}\eta_p\mathbf{c}\cdot\mathbf{v}^p * \left(\alpha_p\mathbf{v}_{\cos}(K_q) + (1-\alpha_p)\mathbf{v}_{\sin}(K_q)\right)(K-K_q)^p + \mathcal{O}\left[(\Omega-\Omega_q)^N + (K-K_q)^I\right] = 0, \tag{16}$$

where

$$\alpha_p = \frac{1+(-1)^p}{2}, \quad \eta_p = \frac{(-1)^{\frac{2p+1+(-1)^{p+1}}{4}}}{p!},$$

that is transformable to the generalization of (10) by substituting $K - K_q = \frac{\Omega-\Omega_q}{\gamma}$ and truncating to $\mathcal{O}(\Omega^N + K^I)$:

$$c_0 + \sum_{p=0}^{N-1}\eta_p\left(\alpha_p\Theta^p_{\cos} + (1-\alpha_p)\Theta^p_{\sin}\right)\Big|_{K-K_q=\frac{\Omega-\Omega_q}{\gamma}} + \sum_{p=N}^{I-1}\eta_p\mathbf{c}\cdot\mathbf{v}^p * \left[\alpha_p\mathbf{v}_{\cos}(K_q) + (1-\alpha_p)\mathbf{v}_{\sin}(K_q)\right](K-K_q)^p = 0. \tag{17}$$

Equating each of the terms in (17) to zero leads to the generalization of (11):

$$c_0 + \cos\Omega_q + \mathbf{c}\cdot\mathbf{v}_{\cos}(K_q) = 0, \quad p = 0, \tag{18a}$$

$$\alpha_p\left(\cos\Omega_q + \frac{\mathbf{c}\cdot\mathbf{v}^p * \mathbf{v}_{\cos}(K_q)}{\gamma^p}\right) + (1-\alpha_p)\left(\sin\Omega_q + \frac{\mathbf{c}\cdot\mathbf{v}^p * \mathbf{v}_{\sin}(K_q)}{\gamma^p}\right) = 0, \quad p = 1,\ldots,N-1, \tag{18b}$$

$$\mathbf{c}\cdot\mathbf{v}^p * \left[\alpha_p\mathbf{v}_{\cos}(K_q) + (1-\alpha_p)\mathbf{v}_{\sin}(K_q)\right] = 0, \quad p = N,\ldots,I-1, \quad N \leqslant I \leqslant M+1. \tag{18c}$$

The usage of Eqs. (11) and (18) can now be summarized as follows. Given the $(3, 2M+1)$ stencil size, we have a total of $M+1$ degrees of freedom in the form of the coefficients $c_m, m = 0,\ldots,M$. The $M+1$ corresponding equations can be partitioned into T groups, each one corresponding to a point $(\Omega_q, K_q), q = 1,\ldots,T$ on the linear dispersion curve such that

$$\sum_{i=1}^{T} I_q = M+1. \tag{19}$$

Recall that at $(\Omega_q, K_q) = (0,0), N, I$ must be even. Then, in (19) replace I_q by $I_q/2$.

At each one of these points, the GDE is made to fit the linear curve to a prescribed $\mathrm{SOoA}_q = (N_q, I_q)$ by invoking one or more of the equations of the system (11) or (18). (11a) is always used to ensure that the GDE intersects with the linear curve at (Ω_q, K_q). This ensures a minimal SOoA of (1,1) at $(\Omega_q, K_q) > (0,0)$ and (2,2) at $(\Omega_q, K_q) = (0,0)$. This employs T out of the total $M+1$ equations. The rest of the equations are in the form of (18b) and (18c), and are used to match derivatives of several orders. This can be done in two ways: (a) usage of equations of the type (18c), that serves to increase the parameter I_q at that point and (b) use of (18c), that increases both I_q and N_q concurrently, being the equivalent of "derivative swapping" technique. One is thus faced with tradeoffs between taking higher order SOoA at a given point vs. lower orders at multiple points across the frequency range. The highest possible value of the SOoA is attained when all equations except the initial T equations are assigned to a single point. If this point is not the origin, then this maximal value is $I_{\max} = M + 2 - T$. If the point is the origin, then $I_{\max} = 2(M + 2 - T)$.

If intersection with the point (0,0) is included with a matching of the first derivative, i.e. SOoA at $(0,0) \geqslant (4,4)$, then the conventional OoA is defined. In this case, the remaining degrees of freedom are utilized for increasing the SOoA at other frequencies. This increase *is equivalent to an independent specification of dispersion error reduction*, as is done, for example, in the context of the non-standard FDTD schemes. The concept of the SOoA is thus seen as encompassing all schemes by consolidating the notions of orders of accuracy and dispersion errors reduction.

2.4. Stability analysis

For stability analysis of these schemes, define the *generalized amplification polynomial* (GAP) in accordance with Von Neumann analysis, as the outcome of Eq. (3), upon substituting $E_i^n = \xi^i(\Delta x)\tau^n(\Delta t)$ with $(\xi, \tau) = (e^{jK}, g)$:

$$g^2 + 2\left(\sum_{m=0}^{M} c_m \cos mK\right) g + 1 = 0. \tag{20}$$

For the scheme to be stable, the necessary requirement is that the roots of (20) obey $|g_{1,2}| \leqslant 1$. This implies the condition

$$\left(\sum_{m=0}^{M} c_m \cos mK\right)^2 \leqslant 1 \quad \forall K \tag{21}$$

that in turn imposes constraints on the coefficients c_m. To find these constraints, one first evaluates the extrema of the left hand side of (21) over K. The non-trivial factor in the derivative expression is

$$\sum_{m=1}^{M} m c_m \sin mK = 0. \tag{22}$$

Substituting the solutions of (22) into (21), one obtains constraints on c_m that translate in turn to criteria for γ and other parameters of the scheme (see definition of Ω_q below). Note that $K = 0, \pi$ is always a solution. The stability criterion needs to be considered concurrently with the equations relating these coefficients obtained from SOoA considerations.

3. One-dimensional case studies

The cases below demonstrate the construction of FDTD schemes according to requirements derived from the spectrum of the excitation. Customarily, different discretization schemes are characterized by the conventional order of accuracy (OoA). For the sake of comparison between schemes, we utilize the concept of size-order (S-O) of an FDTD scheme defined by the 4-number $[alpha_t, \alpha_x; \beta_t, \beta_x]$ to account for (α_t, α_x) stencils sizes and (β_t, β_x) OoA: S-O $= [\underbrace{p_t, p_x}_{\text{Stencil Size}}; \underbrace{q_t, q_x}_{\text{OoA}}]$, e.g. the scheme in (28) below is of S-O [3,3; 2,2]. The (S-O) is used alongside with the SOoA in the examples listed below. In cases where the origin of the dispersion curve is not one of the T points on the curve, the OoA, and hence the S-O of the scheme are not defined. In cases such as these, the comparison is done solely with respect to the stencil size. The examples are listed by ascending stencil size, i.e. (3,3), (3,5) and (3,7). Eqs. (3), (5) and (22) for the generic difference equation, the corresponding GDE and the stability condition, respectively, are specialized for each stencil size. The cases are ordered by the number of specified frequencies T, as defined after (18), and further detailed by all possible SOoAs, specializing (11) whenever $(\Omega_q, K_q) = (0,0)$ or (18) for other frequency points. Stability analysis is carried out analytically for the simpler cases where the cs are functions of γ only. The rest of the cases, where the cs are functions of γ and one or more Ω_qs, are analyzed via what we denote as "stability maps". These maps are drawn based on the stability inequalities and present possible Ω_qs vs. γ which produce schemes satisfying stability criteria.

3.1. (3,3) Stencil

For this stencil size, $2M+1=3$, i.e. $M=1$. Therefore, one can select up to two frequency points (see explanation around (19)), i.e. $T \leqslant 2$. The maximal SOoA is (4,4) and (2,2) for $(\Omega,K)=(0,0)$ and $(\Omega,K)>(0,0)$, respectively. These parameters are summarized in Tables 1 and 2.

Eqs. (3) and (5) for the generic difference equation and corresponding GDE now take the form of (23a) and (23b), respectively:

$$E_i^{n+1}+E_i^{n-1}+2c_0E_i^n+c_1\left(E_{i+1}^n+E_{i-1}^n\right)=0, \tag{23a}$$

$$\cos\Omega+c_0+c_1\cos K=0. \tag{23b}$$

Stability analysis:
Solving (22), now in the form of

$$c_1\sin K=0, \tag{24}$$

we have

$$K=0,\pi \tag{25}$$

as the only solutions. Substituting this result into (21), we have

$$|c_0+c_1|\leqslant 1, \tag{26a}$$

$$|c_0-c_1|\leqslant 1. \tag{26b}$$

Criteria for γ and Ω_q are deduced below.

3.1.1. $T=1$

(a) $(\Omega_1,K_1)=(0,0)$, $\mathrm{SOoA}_1=(4,4)$. Eq. (11) include here the orders $p=0,1$:

$$1+c_0+c_1=0, \tag{27a}$$

$$c_1=-\gamma^2. \tag{27b}$$

Using these coefficients in (23a) we reconstruct the familiar S-O [3,3; 2,2] scheme

$$E_i^{n+1}+E_i^{n-1}+2(\gamma^2-1)E_i^n-\gamma^2\left(E_{i+1}^n+E_{i-1}^n\right)=0, \tag{28}$$

that is second order accurate in time and space.

For stability criterion, merge (28) into (27a). Then (26a) is satisfied automatically, and (26b) becomes

$$|1+2c_1|\leqslant 1 \;\Rightarrow\; -1\geqslant c_1\leqslant 0 \quad\Rightarrow \gamma^2\leqslant 1 \tag{29}$$

which is the familiar Courant–Friedrich–Lewy criterion.

(b) $(\Omega_1,K_1)>(0,0)$, $\mathrm{SOoA}_1=(2,2)$. Eq. (11) are now

$$\cos\Omega_1+c_0+c_1\cos\frac{\Omega_1}{\gamma}=0, \tag{30a}$$

$$c_1=-\frac{\gamma\sin\Omega_1}{\sin\frac{\Omega_1}{\gamma}}. \tag{30b}$$

Table 1
(3,3) Stencil parameters.

M	T	I	
		(0,0)	(Ω_q,K_q)
1	≤ 2	≤ 4	≤ 2

Table 2
(3,5) Stencil parameters.

M	T	I	
		(0,0)	(Ω_q,K_q)
2	≤ 3	≤ 6	≤ 3

This choice of coefficient creates a scheme where the dispersion curve fits the linear curve at the prescribed frequency point (Ω_1, K_1) up to the first derivative at that point. However, the curve does not intersect with the origin, therefore conventional OoA is not defined for this scheme.

For a stability criterion, the scheme is inherently unstable, since it can be shown that for the (3,3) stencil, instability is mandatory if the point (0,0) is not included in the GDE curve.

3.1.2. $T = 2$

(a) $(\Omega_1, K_1) = (0,0), (\Omega_2, K_2) > (0,0), \mathrm{SOoA}_1 = (2,2), \mathrm{SOoA}_2 = (1,1)$. In this case, Eq. (11) are

$$1 + c_0 + c_1 = 0, \tag{31a}$$

$$\cos\Omega_2 + c_0 + c_1 \cos\frac{\Omega_2}{\gamma} = 0, \tag{31b}$$

$$E_i^{n+1} + E_i^{n-1} + 2\frac{\cos\frac{\Omega_2}{\gamma} - \cos\Omega_2}{1 - \cos\frac{\Omega_2}{\gamma}} E_i^n - \frac{1 - \cos\Omega_2}{1 - \cos\frac{\Omega_2}{\gamma}} \left(E_{i+1}^n + E_{i-1}^n\right) = 0. \tag{32}$$

In the scheme (32), the requirement of $\mathrm{SOoA}_2 = (1,1)$ at (Ω_2, K_2) is seen as equivalent to requiring $V_p|_{(\Omega_2,K_2)} = \frac{\Omega_2}{K_2} = \gamma$. The numerical group velocity, however, is not equal to the linear one due to the lack of degrees of freedom. The scheme of (32) coincides with the well-known non-standard FDTD (NSFDTD) scheme [14–18]. For a stability criterion, use (26) with (32). Then, (26a) is satisfied automatically, and (26b) becomes

$$|1 + 2c_1| \leqslant 1 \quad \Rightarrow \quad -1 \leqslant c_1 \leqslant 0, \tag{33}$$

i.e.

$$\cos\Omega_2 \geqslant \cos\frac{\Omega_2}{\gamma} \tag{34}$$

such that $\gamma \leqslant 1$ as long as $\Omega_2 \leqslant \gamma\pi$.

(b) $(\Omega_2, K_2) > (\Omega_1, K_1) > (0,0), \mathrm{SOoA}_1 = \mathrm{SOoA}_2 = (1,1)$. For this case,

$$\cos\Omega_1 + c_0 + c_1 \cos\frac{\Omega_1}{\gamma} = 0, \tag{35a}$$

$$\cos\Omega_2 + c_0 + c_1 \cos\frac{\Omega_2}{\gamma} = 0. \tag{35b}$$

This choice of two frequencies with the minimal SOoA is equivalent to requiring that the GDE curve intersects the linear curve at the two frequencies without equating the derivatives at these points, i.e. $V_{\mathrm{phase}}|_{(\Omega_{1,2},K_{1,2})} = \frac{\Omega_{1,2}}{K_{1,2}} = \gamma$, while the same does not apply to the group velocity. However, similarly to the case of (30), a Von Neumann analysis of this scheme shows that it is unstable.

3.2. (3,5) Stencils

The (3,5) stencil provides additional degrees of freedom compared with the (3,3) case, as shown in Table 1. For example, V_{phase} can be specified at more than one frequency, or the group velocity V_g could be specified by raising the SOoA at any point to the level of (3,3) ((6,6) at the origin).

For the (3,5) stencil, $M = 2$ and the generic scheme of (3) and the corresponding GDE (5) become, respectively,

$$E_i^{n+1} + E_i^{n-1} + 2c_0 E_i^n + c_1\left(E_{i+1}^n + E_{i-1}^n\right) + c_2\left(E_{i+2}^n + E_{i-2}^n\right) = 0, \tag{36a}$$

$$\cos\Omega + c_0 + c_1\cos K + c_2\cos 2K = 0 \tag{36b}$$

or, representing (36b) explicitly,

$$K = \cos^{-1}\left(\frac{-c_1}{4c_2} \pm \sqrt{\left(\frac{c_1}{4c_2}\right)^2 - \frac{c_0 - c_2 + \cos\Omega}{2c_2}}\right). \tag{37}$$

Table 3
(3,7) Stencil parameters.

M	T	I	
		(0,0)	(Ω_q, K_q)
3	≤ 4	≤ 8	≤ 4

Stability analysis:
Eq. (22) now becomes

$$\sin K(c_1 + 4c_2 \cos K) = 0 \Rightarrow K = 0, \pi \quad \text{and} \quad c_1 + 4c_2 \cos K = 0. \tag{38}$$

Assuming that the equation $c_1 + 4c_2 \cos K = 0$ has no real K as a solution, i.e.

$$\left|\frac{c_1}{4c_2}\right| > 1 \tag{39}$$

one is left with the two extreme points at $K = 0, \pi$. Substituting this result into (21), we have

$$|c_0 + c_1 + c_2| \leqslant 1, \tag{40a}$$
$$|-c_0 + c_1 - c_2| \leqslant 1, \tag{40b}$$

from which criteria for γ and Ω_q can be obtained. In the examples below, these criteria are shown alongside with the solutions for the c_ms. For cases with $T = 1$ and $\Omega_1 = 0, K_1 = 0$, where OoA is defined, the stability criterion depends solely on γ. In other cases, the criterion will depend on Ω_q as well as on γ. For each of these cases, areas of stability are shown graphically as shaded areas on a two-dimensional map, with γ and Ω_q serving as the horizontal and vertical axes, respectively.

3.2.1. Case studies

Four different schemes pertaining to $T = 1$, are described in this section. The remaining cases are presented in Appendix A along with stability analyses for these cases.

$T = 1$: The cases $(\Omega_1, K_1) = (0, 0)$:
(a) $\text{SOoA}_1 = (4, 6)$ (b) $\text{SOoA}_1 = (6, 6)$
Eq. (11) becomes, for the respective SOoAs,

$$\begin{pmatrix} 1 & 1 & 1 \\ 0 & 1^2 & 2^2 \\ 0 & 1^4 & 2^4 \end{pmatrix} \cdot \begin{pmatrix} c_0 \\ c_1 \\ c_2 \end{pmatrix} = \underbrace{\begin{pmatrix} -1 \\ -\gamma^2 \\ 0 \end{pmatrix}}_{\text{(a)}}; \underbrace{\begin{pmatrix} -1 \\ -\gamma^2 \\ -\gamma^4 \end{pmatrix}}_{\text{(b)}} \tag{41}$$

such that the differencing scheme of case (a) takes the form

$$\frac{E_i^{n+1} - 2E_i^n + E_i^{n-1}}{\Delta t^2} - c^2 \left[\frac{-\frac{5}{2}E_i^n + \frac{4}{3}\left(E_{i+1}^n + E_{i-1}^n\right) - \frac{1}{12}\left(E_{i+2}^n + E_{i-2}^n\right)}{\Delta x^2}\right] = 0. \tag{42}$$

Eq. (42) coincides with the standard S-O [3,5; 2,4] scheme.

For a stability criterion, use (40) with (41). Then, (40a) is satisfied automatically, and

$$|1 + 2c_1| \leqslant 1 \quad \Rightarrow \quad -1 \leqslant c_1 \leqslant 0 \tag{43}$$

hence the well known result

$$-1 \leqslant -\frac{4}{3}\gamma^2 \leqslant 0 \quad \Rightarrow \quad \gamma \leqslant \frac{\sqrt{3}}{2}. \tag{44}$$

The resultant discretization scheme for case (b) is

$$\frac{\frac{\gamma^2-4}{2}E_i^n + E_i^{n+1} + E_i^{n-1}}{\Delta t^2} - c^2 \left[\frac{\frac{\gamma^2-4}{2}E_i^n + \frac{4-\gamma^2}{3}\left(E_{i+1}^n + E_{i-1}^n\right) + \frac{\gamma^2-1}{12}\left(E_{i+2}^n + E_{i-2}^n\right)}{\Delta x^2}\right] = 0. \tag{45}$$

The temporal OoA has been raised to 4,[1] i.e. this scheme is of S-O [3,5; 4,4], effectively using the principle of derivative swapping technique [5]. Note that the gain in OoA can come at the expense of reducing the grid cutoff frequency.

For stability, use (40) with (41). Then, (40a) is satisfied automatically, and

$$|1 + 2c_1| \leqslant 1 \quad \Rightarrow \quad -1 \leqslant c_1 \leqslant 0 \tag{46}$$

or

$$-1 \leqslant -\frac{4 - \gamma^2}{3}\gamma^2 \leqslant 0 \quad \Rightarrow \quad \gamma \leqslant 1 \tag{47}$$

as may be expected with a higher order method.

The following schemes are listed for completeness only (see Fig. 1).
$T = 1$: The cases $(\Omega_1, K_1) > (0, 0)$:
(c) $\text{SOoA}_1 = (2, 3)$ (d) $\text{SOoA}_1 = (3, 3)$

[1] Note that the temporal order of the difference equation remains 2, having used three consecutive temporal samples in the scheme.

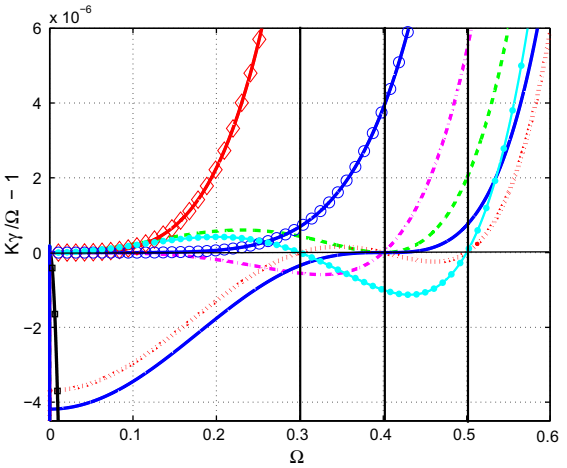

Fig. 1. Dispersion curves of $K\gamma/\Omega - 1$ for some of the (3,7) stencil schemes. $T = 1$ (Section 3.3.1): solid (black) line with squares: (a); solid (red) line with diamonds: (b); solid (blue) line with circles: (c). $T = 2$ (Section B.1): dashed-dotted (magenta) line: (c); dashed (green) line: (g); solid (blue) line: (j). $T = 3$ (Section B.2): solid cyan with filled circles: (b). $T = 4$ (Section B.3): Thin dotted (red) line (a). The vertical scale is blown up to show the differences between the schemes. These differences, although seemingly small, have a large impact on long term errors. (For interpretation of the references to colour in this figure legend, the reader is referred to the web version of this article.)

Eq. (18) becomes, for the respective SOoAs,

$$\begin{pmatrix} 1 & \cos K_1 & \cos 2K_1 \\ 0 & \sin K_1 & \sin 2K_1 \\ 0 & \cos K_1 & \cos 2K_1 \end{pmatrix} * \begin{pmatrix} 1 & 1 & 1 \\ 0 & 1 & 2 \\ 0 & 1^2 & 2^2 \end{pmatrix} \cdot \begin{pmatrix} c_0 \\ c_1 \\ c_2 \end{pmatrix} = \begin{pmatrix} \cos \Omega_1 \\ \sin \Omega_1 \\ \cos \Omega_1 \end{pmatrix} * \underbrace{\begin{pmatrix} -1 \\ -\gamma \\ 0 \end{pmatrix}}_{(c)} ; \underbrace{\begin{pmatrix} -1 \\ -\gamma \\ -\gamma^2 \end{pmatrix}}_{(d)}, \tag{48}$$

where the symbol * denotes the matrix Hadamard product (see definition for the vector Hadamard product in conjunction with (13)). To date, schemes with $(\Omega_1, K_1) > (0,0)$ do not have documented counterparts. These two cases have stable regions in the $\Omega_1 - \gamma$ plane, as shown in Fig. 2(a) and (b), respectively.

For the cases $2 \leqslant T \leqslant 3$ see Appendix A.

3.3. (3,7) Stencils

The available degrees of freedom for this stencil are summarized in Table 3. Here, the generic scheme of (3) and the corresponding GDE become, respectively,

$$E_i^{n+1} + E_i^{n-1} + 2c_0 E_i^n + c_1 (E_{i+1}^n + E_{i-1}^n) + c_2 (E_{i+2}^n + E_{i-2}^n) + c_3 (E_{i+3}^n + E_{i-3}^n) = 0, \tag{49a}$$

$$\cos \Omega + c_0 + c_1 \cos K + c_2 \cos 2K + c_3 \cos 3K = 0. \tag{49b}$$

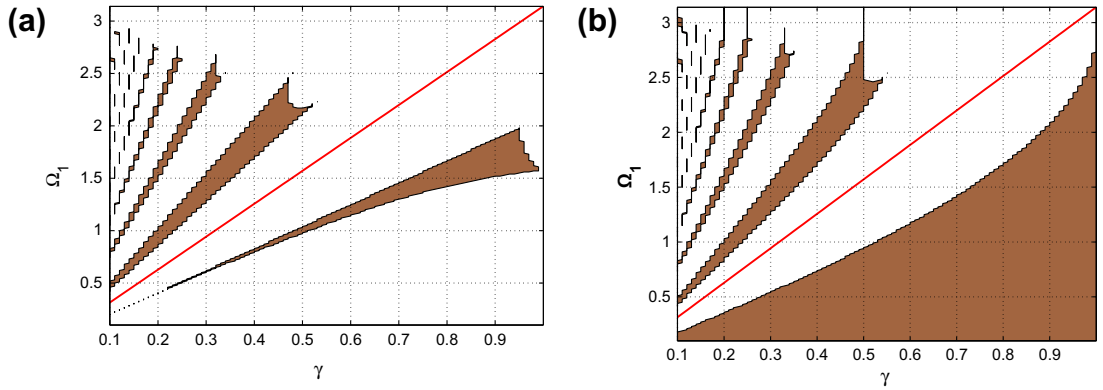

Fig. 2. Stability maps, showing areas of possible stable schemes for Section 3.2.1 ((3,5) stencil, $T = 1$). (a) Case (c) (SOoA $= (2,3)$), (b) case (d) (SOoA $= (3,3)$), where $\Omega_1 > 0$ is in the range $(0.1, \pi)$ and $0.1 < \gamma < 1$. Shaded (brown) areas are the islands of stability. The relevant region below cutoff is seen below the solid (red) line. (For interpretation of the references to colour in this figure legend, the reader is referred to the web version of this article.)

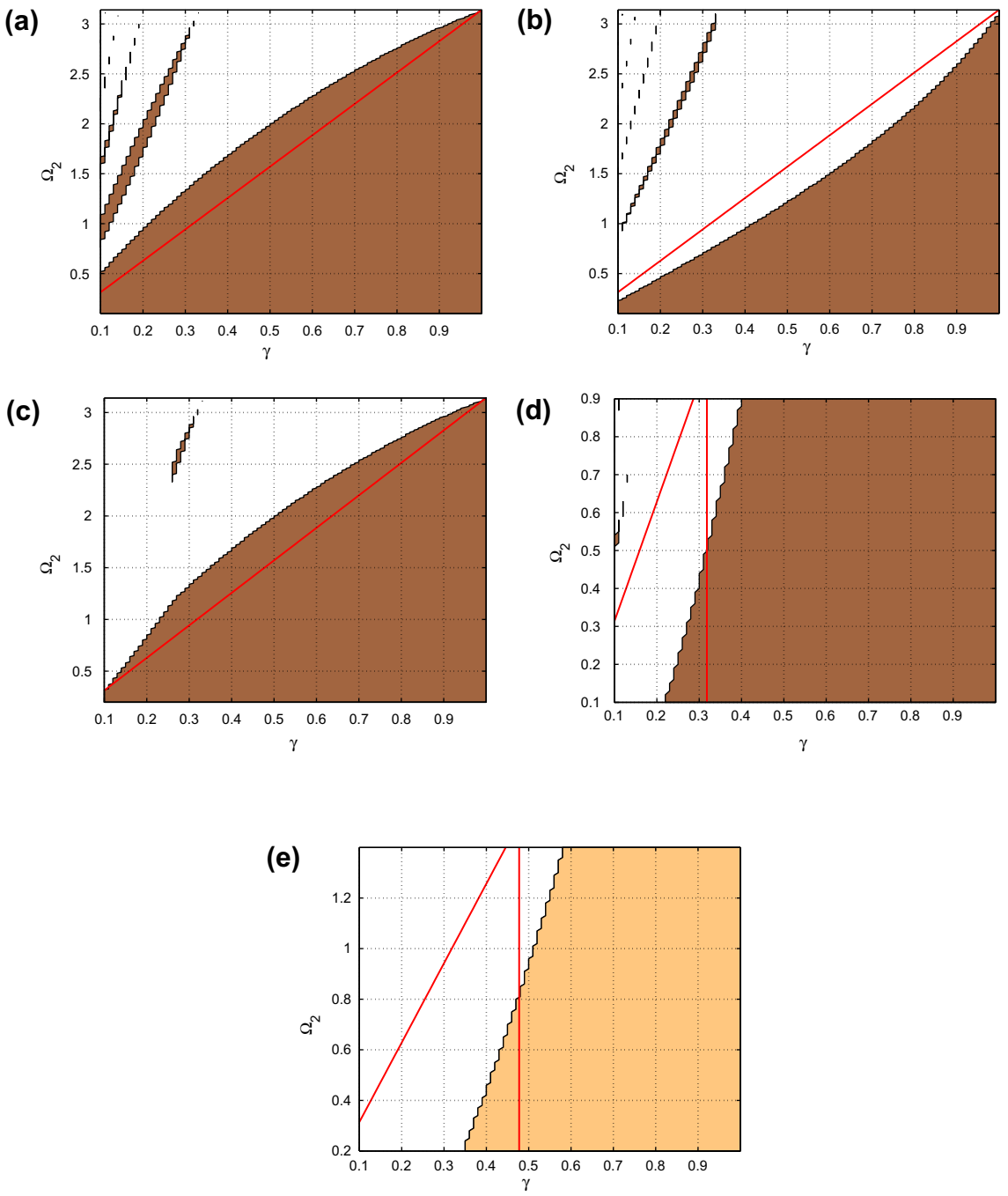

Fig. 3. Stability maps, showing areas of possible stable schemes. Section A.1 (3,5) stencil, $T = 2$: (a) Case (b) ($\mathrm{SOoA}_1 = (4,4), \mathrm{SOoA}_2 = (1,1), \Omega_1 = 0$), (b) case (d) ($\mathrm{SOoA}_1 = (2,2), \mathrm{SOoA}_2 = (2,2), \Omega_1 = 0$), (c) case (f') ($\mathrm{SOoA}_1 = (2,2), \mathrm{SOoA}_2 = (1,1), \Omega_1 = 0.1$). Section A.2 (3,5) stencil, $T = 3, \Omega_1 = 0, \Omega_3 = 1$: (d) case (a) ($\mathrm{SOoA}_1 = (2,2), \mathrm{SOoA}_2 = \mathrm{SOoA}_3 = (1,1)$), (e) case (b) ($\mathrm{SOoA}_1 = \mathrm{SOoA}_1 = \mathrm{SOoA}_1 = (1,1)$); $0.1 < \gamma < 1$. Shaded (brown) areas are the islands of stability. The relevant region below cutoff is seen below the solid (red) line. (For interpretation of the references to colour in this figure legend, the reader is referred to the web version of this article.)

For an explicit representation, rewrite (49b) as

$$\cos^3 K + \frac{c_2}{2c_3}\cos^2 K + \frac{c_1 - 3c_3}{4c_3}\cos K + \frac{\cos\Omega + c_0 - c_2}{4c_3} = 0 \tag{50}$$

and define

$$X=\cos K,\quad \alpha_1=\frac{c_2}{2c_3},\quad \alpha_2=\frac{c_1-3c_3}{4c_3},\quad \alpha_3=\frac{\cos\Omega+c_0-c_2}{4c_3}$$

to obtain

$$X^3+\alpha_1X^2+\alpha_2X+\alpha_3=0. \tag{51}$$

Define also

$$Q=\frac{3\alpha_2-\alpha_1^2}{9},\quad R=\frac{9\alpha_1\alpha_2-27\alpha_3-2\alpha_1^3}{54},\quad S=\sqrt[3]{R+\sqrt{Q^3+R^2}},\quad T=\sqrt[3]{R-\sqrt{Q^3+R^2}}$$

arriving at the following explicit representation of (49b):

$$K=\cos^{-1}\left(S+T-\frac{1}{3}\alpha_1\right). \tag{52}$$

Stability analysis:
Invoking (22),

$$c_1\sin K+2c_2\sin 2K+3c_3\sin 3K=0 \tag{53}$$

the outcome is

$$K=0,\pi\quad\text{and}\quad 12c_3\cos^2K+4c_2\cos K+c_1-3c_3=0. \tag{54}$$

Assume now that the equation $12c_3\cos^2K+4c_2\cos K+c_1-3c_3=0$ has no real K as a solution. Then,

$$12c_3\cos^2K+4c_2\cos K+c_1-3c_3=0\Rightarrow\cos K_{1,2}=\frac{-\frac{c_2}{3c_3}\pm\sqrt{\left(\frac{c_2}{3c_3}\right)^2-\frac{c_1-3c_3}{3c_3}}}{2}. \tag{55}$$

K will not be a real if either condition in (56a) is met:

$$|\cos K_{1,2}|>1, \tag{56a}$$

$$\left(\frac{c_2}{3c_3}\right)^2-\frac{c_1-3c_3}{3c_3}<0 \tag{56b}$$

then we are left with the two extrema points $K=0,\pi$. We need to impose $|b|\leqslant 1$ and substituting these points in to b we arrive at the two inequalities:

$$|c_0+c_1+c_2+c_3|\leqslant 1, \tag{57a}$$

$$|-c_0+c_1-c_2+c_3|\leqslant 1. \tag{57b}$$

3.3.1. Case studies

The (3,7) stencil provides a foundation for many schemes, see representative dispersion curves in Fig. 1, out of which six different schemes pertaining to $T=1$, are described herein. Twenty four more examples are given in Appendix B along with a stability summary in Table B.1. Fourteen out of the thirty schemes where found to have stability regions.

$T=1$: The cases $(\Omega_1,K_1)=(0,0)$:
(a) $\mathrm{SOoA}_1=(4,8)$ (b) $\mathrm{SOoA}_1=(6,8)$ (c) $\mathrm{SOoA}_1=(8,8)$
Eq. (11) becomes, for the respective SOoAs,

$$\begin{pmatrix}1&1&1&1\\0&1^2&2^2&3^2\\0&1^4&2^4&3^4\\0&1^6&2^6&3^6\end{pmatrix}\cdot\begin{pmatrix}c_0\\c_1\\c_2\\c_3\end{pmatrix}=\underbrace{\begin{pmatrix}-1\\-\gamma^2\\0\\0\end{pmatrix}}_{(a)};\underbrace{\begin{pmatrix}-1\\-\gamma^2\\-\gamma^4\\0\end{pmatrix}}_{(b)};\underbrace{\begin{pmatrix}-1\\-\gamma^2\\-\gamma^4\\-\gamma^6\end{pmatrix}}_{(c)}. \tag{58}$$

The solutions, defined as $\mathbf{c}^{(N,8)}=\left(c_0^{(N,8)}\ c_1^{(N,8)}\ c_2^{(N,8)}\ c_3^{(N,8)}\right);N=4,6,8$, are

$$\begin{pmatrix}\mathbf{c}^{(4,8)}\\\mathbf{c}^{(6,8)}\\\mathbf{c}^{(8,8)}\end{pmatrix}=\begin{pmatrix}-1&0&0&0\\&\mathbf{c}^{(4,8)}&\\&\mathbf{c}^{(6,8)}&\end{pmatrix}+\begin{pmatrix}\gamma^2&0&0\\0&\gamma^4&0\\0&0&\gamma^6\end{pmatrix}\begin{pmatrix}\frac{49}{36}&-\frac{3}{2}&\frac{3}{20}&-\frac{1}{90}\\-\frac{7}{18}&\frac{13}{24}&-\frac{1}{6}&\frac{1}{72}\\\frac{1}{36}&-\frac{1}{24}&\frac{1}{60}&-\frac{1}{360}\end{pmatrix}. \tag{59}$$

These coefficients produce S-O [3,7; 2,6], [3,7; 4,6] and [3,7; 6,6] schemes, respectively.

$T=1$: The cases $(\Omega_1,K_1)>(0,0)$:
(d) $\mathrm{SOoA}_1=(2,4)$ (e) $\mathrm{SOoA}_1=(3,4)$ (f) $\mathrm{SOoA}_1=(4,4)$

Eq. (18) becomes, for the respective SOoAs,

$$\begin{pmatrix} 1 & \cos K_1 & \cos 2K_1 & \cos 3K_1 \\ 0 & \sin K_1 & \sin 2K_1 & \sin 3K_1 \\ 0 & \cos K_1 & \cos 2K_1 & \cos 3K_1 \\ 0 & \sin K_1 & \sin 2K_1 & \sin 3K_1 \end{pmatrix} * \begin{pmatrix} 1 & 1 & 1 & 1 \\ 0 & 1 & 2 & 3 \\ 0 & 1^2 & 2^2 & 3^2 \\ 0 & 1^3 & 2^3 & 3^3 \end{pmatrix} \cdot \begin{pmatrix} c_0 \\ c_1 \\ c_2 \\ c_3 \end{pmatrix} = \begin{pmatrix} \cos\Omega_1 \\ \sin\Omega_1 \\ \cos\Omega_1 \\ \sin\Omega_1 \end{pmatrix} * \underbrace{\begin{pmatrix} -1 \\ -\gamma \\ 0 \\ 0 \end{pmatrix}}_{(d)} ; \underbrace{\begin{pmatrix} -1 \\ -\gamma \\ -\gamma^2 \\ 0 \end{pmatrix}}_{(e)} ; \underbrace{\begin{pmatrix} -1 \\ -\gamma \\ -\gamma^2 \\ -\gamma^3 \end{pmatrix}}_{(f)} . \tag{60}$$

Since $(\Omega_1, K_1) > (0,0)$, the S-O is not defined for this case.

For the cases $2 \leqslant T \leqslant 4$ refer to Appendix B.

4. One-dimensional example

The example below pertains to the (3,5) stencil case (Section 3.2). We choose $\gamma = 0.8$ and use a modulated pulse of the form

$$P(n) = \begin{cases} \cos(\Omega_{\text{mod}} n)\sin^8\left(\frac{\pi n}{200}\right), & 0 \leqslant n \leqslant 200, \\ 0, & \text{elsewhere}, \end{cases} \tag{61}$$

whose spectrum is centered around $\Omega_{\text{mod}} = 0.4$ as shown in Fig. 4. The pulse is shown vs. position at 250,000 and one million time steps in Figs. 5(a) and (b), respectively. The scheme with $T = 2, \Omega_1 = 0,\ \Omega_2 = 0.4, \text{SOoA}_{1,2} = (2,2)$ (Section A.1, case (d)) is compared with the analytical solution and with the standard S-O [3,5; 4,4] scheme where $T = 1, \Omega_1 = 0, \text{SOoA}_1 = (6,6)$ (Section 3.2.1, case (b)). Both schemes, based on the same stencil size, require the same number of algebraic manipulations. The severe effect of the numerical dispersion in the standard scheme is clearly visible, while the improved scheme virtually reproduces the analytical solution at 250,000 time steps and still tracks the center of the analytical solution at a million time steps. The higher accuracy has thus been achieved without an extra computational cost since it is designed for the given pulse spectrum only.

5. The SOoA-based methodology in two-dimensional schemes

5.1. The GDE and the SOoA in two dimensions

The SOoA-based methodology, as introduced in Section 2, is comprised of the following basic steps, that apply equally well to the two-dimensional case described next: (a) formulation of a generic difference equation, given a stencil structure, with undetermined degrees of freedom, (b) transformation of this equation into the spectral domain to form the GDE, and (c) expansion of the GDE into a Taylor series about an arbitrary number of frequency points where the GDE fits the linear dispersion relationship to a specified spectral order of accuracy (SOoA). In applying these steps to the two-dimensional case, features such as anisotropy and the additional complexity of the two- dimensional grid are taken into account.

The two-dimensional GDE can be formulated either in the Cartesian (Ω, K_x, K_y) or polar (Ω, K, ϕ) spectral coordinates, interrelated by

$$K_x = \tilde{k}_x \Delta x = \tilde{k}\Delta x \cos\phi = K\cos\phi, \tag{62a}$$

$$K_y = \tilde{k}_y \Delta y = \tilde{k}\Delta y \sin\phi = rK\sin\phi \tag{62b}$$

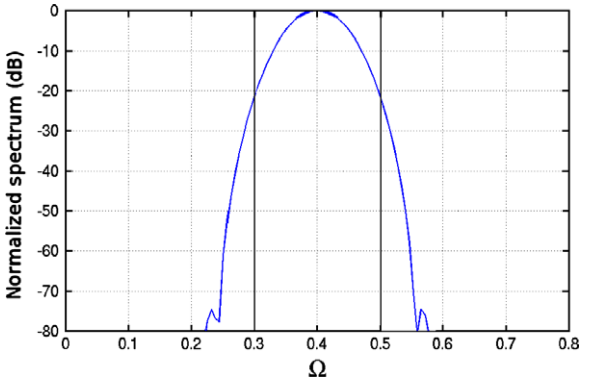

Fig. 4. Spectrum of the exciting pulse (61) vs. frequency of an FDTD grid. Central, lower and upper frequencies are defined as $\Omega = 0.4, 0.3$ and 0.5, respectively.

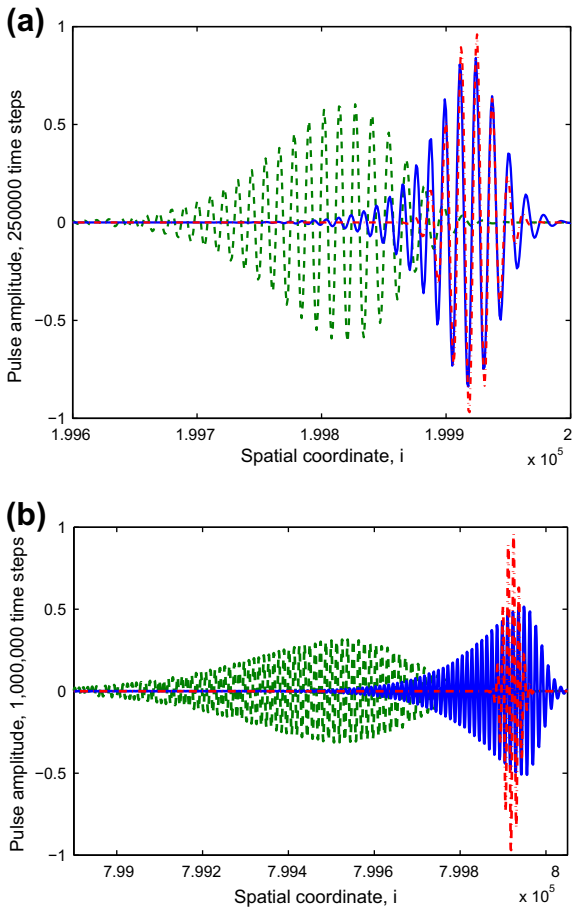

Fig. 5. Snapshot of the pulse of (61) vs. position at (a) 250,000 and (b) one million time steps. Dashed-dotted (red) line: analytical solution; dashed (green) line: $T = 1, \Omega_1 = 0, \mathrm{SOoA}_1 = (6,6)$ (Section 3.2.1, case (b)); solid (blue) line: result of scheme with $T = 2, \Omega_1 = 0,\ \Omega_2 = 0.4, \mathrm{SOoA}_{1,2} = (2,2)$ (Section A.1, case (d)). $\gamma = 0.8$. (For interpretation of the references to colour in this figure legend, the reader is referred to the web version of this article.)

with $r \triangleq \frac{\Delta y}{\Delta x}$. The two-dimensional linear dispersion relation, being the analog of (6), can be written in the Cartesian and polar options, respectively, as

$$-\Omega^2 + \left(\gamma_x^2 K_x^2 + \gamma_y^2 K_y^2\right) = 0, \tag{63a}$$

$$-\Omega^2 + \gamma_x^2 K^2 = 0, \tag{63b}$$

where $\gamma_{x,y} = c\frac{\Delta t}{\Delta x,y}$. Eq. (63b) is an outcome of (63a) using $r = \frac{\Delta y}{\Delta x}$.

The spectral constituent (K_x, K_y) propagates within the i,j grid along the θ direction, while in the physical $i\Delta x, j\Delta y$ space, the propagation is along ϕ, where

$$\frac{K_y}{K_x} = \tan\theta = r\tan\phi. \tag{64}$$

The two-dimensional SOoA is defined in an analogous manner to the one-dimensional SOoA of Section 2. The point about which the GDE is expanded can be defined either in the Cartesian or polar coordinate system, leading to corresponding definitions of the SOoA. For the Cartesian form we denote $\mathrm{SOoA}_q = (N_q, I_{xq}, I_{yq})$ and $P_q = (\Omega_q, K_{xq}, K_{yq})$, residing on the linear dispersion relation surface (63a). In the polar case, $\mathrm{SOoA}_{\phi q} = (N_q, I_q, I_{\phi q})$. and $P_{\phi q} = (\Omega_q, K_q, \phi_q)$, residing on (63b).

5.2. Classification of two-dimensional stencils

Unlike the one-dimensional case, the size portion of the size-order (S-O) concept (see Section 3) in the two-dimensional case should be specified in terms of the stencil structure in the (x,y) plane rather than just by its total number of points. Define a local $(x' = \pm i'\Delta x, y' = \pm j'\Delta y)$ coordinate system centered about the point (i,j), i.e. $x = (i \pm i')\Delta x, y = (j \pm j')\Delta y$ (see Fig. 6). Derivatives are to be approximated as a weighted summation of the points within the stencil centered about (i,j). In the sequel, we focus on stencils with symmetrical properties only.

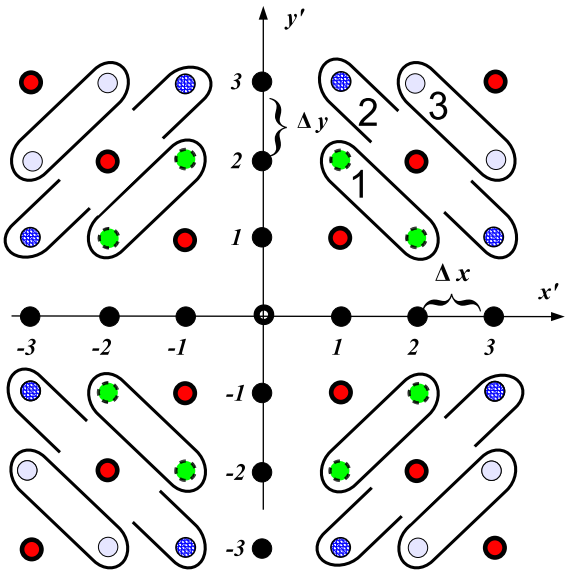

Fig. 6. 2-D Stencil map.

Examining the stencil map in Fig. 6, one can define groups of stencil structures as follows. The first group is comprised of points residing symmetrically on the local coordinate system axes, shown in solid discs in Fig. 6. These stencils have $2M+1$ points, $M=1,2,\ldots$. The number of points over both axes is chosen here to be the same. For this group, the stencil size is denoted as $(3,2M+1,0,0)$ (the temporal stencil size is always 3, and the extra two zeros serve as placeholders for now). The total number of spatial points in the stencil becomes $4M+1$.

The second group incorporates the points of the first group plus points that reside on the two principal diagonals, shown as red discs with solid boundary in Fig. 6. The stencil size for members of this group is denoted $(3,2M+1,D_4,0)$, where the parameter D_4 is the number of sets of points, each set having four points complying with $i'=j'=1,\ldots,D_4$. This adds $4D_4$ points to the total number of points in the first group, rendering the total number of point equal to $4(M+D_4)+1$.

Points lying on secondary diagonals, when added to the points of the second group, form the third group. The size of this group is now denoted $(3,2M+1,D_4,D_8)$. The additional parameter for this group, D_8, counts for the number of sets with 8 points each. In Fig. 6, these sets are encircled and marked with numbers 1–3. $D_8=M_s$ means the incorporation of groups #1 through $\#M_s$. Each set is characterized by $i'^2+j'^2=\text{const}$. For this group, the total number of stencil points is $4(M+D_4+2D_8)+1$.

Fig. 7(a)–(f) depict, respectively, the examples with stencil sizes of: (a) (3,3,0,0), i.e. $M=1,\ D_4=0,\ D_8=0$, (b) (3,5,0,0), i.e. $M=2,D_4=0,D_8=0$, (c) (3,3,1,0), i.e. $M=1,D_4=1,D_8=0$, (d) (3,7,0,0), i.e. $M=3,D_4=0,D_8=0$, (e) (3,5,1,1), i.e. $M=2,D_4=1,D_8=1$ and (f) (3,5,2,1).

5.3. (3,3,0,0) Stencils with $\Delta y\neq\Delta x$

The generic scheme for the (3,3,0,0) stencils is:

$$E_{ij}^{n+1}+E_{ij}^{n-1}+2c_0E_{ij}^{n}+c_1^{x}\left(E_{i+1,j}^{n}+E_{i-1,j}^{n}\right)+c_1^{y}\left(E_{i,j+1}^{n}+E_{i,j-1}^{n}\right)=0, \tag{65}$$

where $x=i\Delta x, y=j\Delta y$ and $t=n\Delta t$. The corresponding Cartesian GDE is

$$\cos\Omega+c_0+c_1^{x}\cos K_x+c_1^{y}\cos K_y=0. \tag{66}$$

In order to fit the GDE surface to the linear dispersion surface up to a specified order, we expand (66) about a point $P_q=(\Omega_q,K_{xq},K_{yq})\neq(0,0,0)$ residing on the linear surface (63a) (see the 1-D analog in Section 2.3) as

$$\begin{aligned}
&\cos\Omega+c_0+c_1^{x}\cos K_x+c_1^{y}\cos K_y\\
&\quad=\cos\Omega_q+c_0+c_1^{x}\cos K_{xq}+c_1^{y}\cos K_{yq}-\sin\Omega_q(\Omega-\Omega_q)-(K_x-K_{xq})c_1^{x}\sin K_{xq}-(K_y-K_{yq})c_1^{y}\sin K_{yq}\\
&\qquad-\frac{1}{2}\cos\Omega_q(\Omega-\Omega_q)^2-\frac{1}{2}(K_x-K_{xq})^2c_1^{x}\cos K_{xq}-\frac{1}{2}(K_y-K_{yq})^2c_1^{y}\cos K_{yq}\frac{1}{3!}\sin\Omega_q(\Omega-\Omega_q)^3\\
&\qquad+\frac{1}{3!}(K_x-K_{xq})^3c_1^{x}\sin K_{xq}+\frac{1}{3!}(K_y-K_{yq})^3c_1^{y}\sin K_{yq}+\cdots=0,
\end{aligned} \tag{67}$$

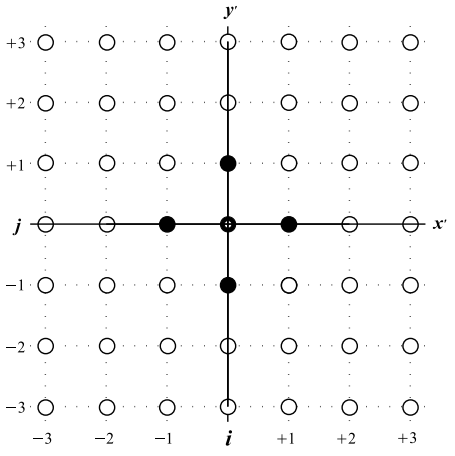

(a) (3 3 0 0)

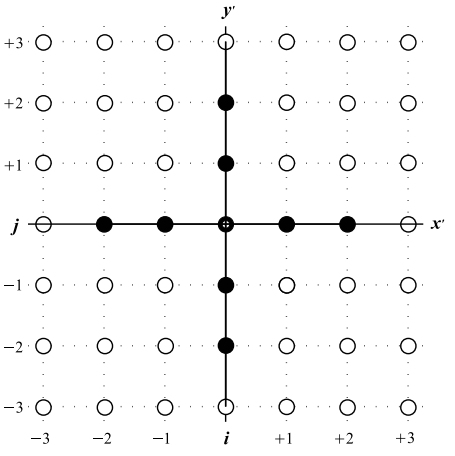

(b) (3 5 0 0)

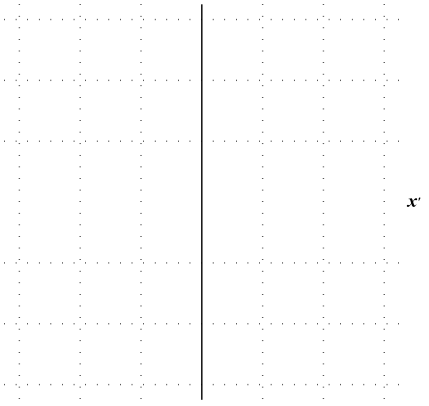

truncate the series to the required order and tune the c values to make the truncated series fit the linear surface. In order to achieve SOoA $= (2, 2, 2)$ at P_q extract the zeroth and first order terms in $(K_x - K_{xq})$ and $(K_y - K_{yq})$ and equate them individually to zero, i.e.

$$\cos\Omega_q + c_0 + c_1^x \cos K_{xq} + c_1^y \cos K_{yq} = 0, \tag{68a}$$

$$\frac{\sin\Omega_q}{\Omega_q}\gamma_x^2 K_{xq} + c_1^x \sin K_{xq} = 0, \tag{68b}$$

$$\frac{\sin\Omega_q}{\Omega_q}\gamma_y^2 K_{yq} + c_1^y \sin K_{yq} = 0, \tag{68c}$$

where (68b) and (68c) have been obtained by setting the first order terms in (67) to zero. The result is

$$c_1^x = -\gamma_x^2 \frac{\sin\Omega_q}{\Omega_q}\frac{K_{xq}}{\sin K_{xq}}, \quad c_1^y = -\gamma_y^2 \frac{\sin\Omega_q}{\Omega_q}\frac{K_{yq}}{\sin K_{yq}} \tag{69}$$

with c_0 obtainable from (68a).

The usage of the polar representation (63b) is considered preferable, though, for the following two reasons: firstly, The GDE as expressed in (63b) is inherently linear, similarly to the one-dimensional case, therefore the linear system for the cs is more easily derived. Secondly, for a given ϕ_q, the results and insights obtained in Section 2 for the one-dimensional case become relevant for that direction.

The GDE written in polar terms is

$$\cos\Omega + c_0 + c_1^x \cos(K\cos\phi) + c_1^y \cos(rK\sin\phi) = 0. \tag{70}$$

Upon expanding (70) about $P_{\phi q} = (\Omega_q, K_q, \phi_q)$, we have

$$\begin{aligned}
&\cos\Omega + c_0 + c_1^x \cos(K\cos\phi) + c_1^y \cos(rK\sin\phi)\\
&= \cos\Omega_q + c_0 + c_1^x \cos(K_q\cos\phi_q) + c_1^y \cos(rK_q\sin\phi_q) - \sin\Omega_q(\Omega-\Omega_q) - (K-K_q)\left[c_1^x \sin(K_q\cos\phi_q)\cos\phi_q\right.\\
&\left.+c_1^y \sin(rK_q\sin\phi_q) r\sin\phi_q\right] - (\phi-\phi_q)\left[c_1^y \sin(rK_q\sin\phi_q) rK_q\cos\phi_q - c_1^x \sin(K_q\cos\phi_q)K_q\sin\phi_q\right]\\
&-\frac{1}{2}\cos\Omega_q(\Omega-\Omega_q)^2 - \frac{1}{2}(K-K_q)^2\left[c_1^x \cos(K_q\cos\phi_q)\cos^2\phi_q + c_1^y \cos(rK_q\sin\phi_q) r^2\sin^2\phi_q\right]\\
&-\frac{1}{2}(\phi-\phi_q)^2\left\{c_1^x\left[\cos(K_q\cos\phi_q)K_q^2\sin^2\phi_q - \sin(K_q\cos\phi_q)K_q\cos\phi_q\right]\right.\\
&\left.+c_1^y\left[\cos(rK_q\sin\phi_q) r^2K_q^2\sin^2\phi_q - \sin(rK_q\sin\phi_q) rK_q\sin\phi_q\right]\right\}\\
&-(K-K_q)(\phi-\phi_q)\left\{c_1^y\left[\cos(rK_q\sin\phi_q) r^2K_q\sin\phi_q\cos\phi_q + \sin(rK_q\sin\phi_q) r\cos\phi_q\right]\right.\\
&\left.-c_1^x\left[\cos(K_q\cos\phi_q)K_q\sin\phi_q\cos\phi_q + \sin(K_q\cos\phi_q)\sin\phi_q\right]\right\} + \cdots = 0.
\end{aligned} \tag{71}$$

Satisfying (71) to first order is quite straightforward (as opposed to the Cartesian case (67))

$$c_1^y \sin(rK_q\sin\phi_q) rK_q\cos\phi_q - c_1^x \sin(K_q\cos\phi_q)K_q\sin\phi_q = 0, \tag{72a}$$

$$c_1^x \sin(K_q\cos\phi_q)\cos\phi_q + c_1^y \sin(rK_q\sin\phi_q) r\sin\phi_q = -\gamma_x\sin\Omega_q \tag{72b}$$

resulting in

$$c_1^x = -\gamma_x \frac{\sin\Omega_q\cos\phi_q}{\sin(K_q\cos\phi_q)}, \quad c_1^y = -\frac{\gamma_x}{r}\frac{\sin\Omega_q\sin\phi_q}{\sin(rK_q\sin\phi_q)}. \tag{73}$$

One can show that (73) is identical to (69).

Stability analysis:

The general amplification polynomial (GAP) is

$$g^2 + 2\underbrace{\{c_0 + c_1^x\cos K_x + c_1^y\cos K_y\}}_{b} g + 1 = 0. \tag{74}$$

Solving the system

$$\frac{\partial(b^2)}{\partial K_x} = -2b\left[c_1^x \sin K_x\right] = 0, \tag{75a}$$

$$\frac{\partial(b^2)}{\partial K_y} = -2b\left[c_1^y \sin K_y\right] = 0 \tag{75b}$$

we have the four extrema $(K_x, K_y) = (0,0), (0,\pi), (\pi,0), (\pi,\pi)$, leading to the system of four inequalities that have to be satisfied simultaneously:

$$-1 \leqslant c_0 + c_1^x + c_1^y \leqslant 1, \tag{76a}$$
$$-1 \leqslant c_0 + c_1^x - c_1^y \leqslant 1, \tag{76b}$$
$$-1 \leqslant c_0 - c_1^x + c_1^y \leqslant 1, \tag{76c}$$
$$-1 \leqslant c_0 - c_1^x - c_1^y \leqslant 1. \tag{76d}$$

Scheme anisotropy analysis:
Rewrite first the dispersion relation seen in Eq. (70):

$$\cos\Omega = -\left[c_0 + c_1^x \cos(K\cos\phi) + c_1^y \cos(rK\sin\phi)\right]. \tag{77}$$

Note that the right hand side of (77) is the same for $\pm\phi$ and $\pm\phi + \pi$ (see solid lines in Fig. 8). Define the error ΔK as the difference between the right hand side of (77) and $\cos(\gamma_x K)$:

$$\Delta K = -\left[c_0 + c_1^x \cos(K\cos\phi) + c_1^y \cos(rK\sin\phi) + \cos(\gamma_x K)\right] \tag{78}$$

the extrema of which contain two solutions that are independent of the coefficients, i.e. $\phi = 0$ and $\phi = \frac{\pi}{2}$. Additional solutions that are coefficient dependent also can be found as shown for various schemes treated below. These help devise schemes with specific requirements related to anisotropy.

5.3.1. $T = 1$

We now proceed to survey schemes that are based on the expansion of the GDE about a single point P_1 in the spectral domain. Consider two cases: (1) the conventional case where $P_1 = (\Omega_1 = 0, K_{x1} = 0, K_{y1} = 0)$ is at the origin and (2) $P_1 = (\Omega_1, K_{x1}, K_{y1})$, $\Omega_1 \neq 0$.

Case (1): $P_1 = (\Omega_1 = 0, K_{x1} = 0, K_{y1} = 0)$

This case coincides with the standard S-O [3,3; 2,2] FDTD scheme.

Cartesian formulation:

Apply $\Omega_1 = K_{x1} = K_{y1} = 0$ to (67):

$$\cos\Omega + c_0 + c_1^x \cos K_x + c_1^y \cos K_y = 1 + c_0 + c_1^x + c_1^y - \frac{1}{2}\Omega^2 - \frac{1}{2}K_x^2 c_1^x - \frac{1}{2}K_y^2 c_1^y + \mathcal{O}\left(\Omega^4 + K_x^4 + K_y^4\right) = 0, \tag{79}$$

i.e.

$$1 + c_0 + c_1^x + c_1^y = 0, \tag{80a}$$
$$c_1^x = -\gamma_x^2, \tag{80b}$$
$$c_1^y = -\gamma_y^2 \tag{80c}$$

with the resultant SOoA of (4,4,4) that is synonymous with the standard S-O of [3,3; 2,2].

Polar formulation:

In this case we use Eq. (71) with $(\Omega_q, K_q, \phi_q) = (0, 0, \phi_q)$:

$$\begin{aligned}&\cos\Omega + c_0 + c_1^x \cos(K\cos\phi) + c_1^y \cos(rK\sin\phi)\\ &\quad = 1 + c_0 + c_1^x + c_1^y - \frac{1}{2}\Omega^2 - \frac{1}{2}K^2\left[c_1^x \cos^2\phi_q + c_1^y r^2 \sin^2\phi_q\right] + \mathcal{O}(\Omega^4 + K^4 + \phi^4) = 0.\end{aligned} \tag{81}$$

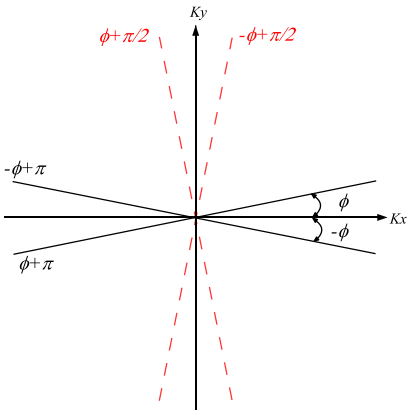

Fig. 8. Symmetry of anisotropy in ϕ.

Equating (81) to (63b) up to second order in Ω and K we have, for all ϕ_q

$$1 + c_0 + c_1^x + c_1^y = 0, \tag{82a}$$

$$c_1^x \cos^2\phi_q + c_1^y r^2 \sin^2\phi_q = -\gamma_x^2 \ \ \forall\phi_q \tag{82b}$$

leading to the replication of (80):

$$c_1^x = c_1^y r^2 = -\gamma_x^2. \tag{83}$$

Application of the stability analysis (76) produces the well known CFL condition:

$$\gamma_x^2 + \gamma_y^2 \leqslant 1. \tag{84}$$

Anisotropy analysis (see paragraph after (78)) shows that in addition to $\phi = 0$ and $\phi = \frac{\pi}{2}$, we have an extremum for the anisotropy error at

$$\tan\phi_0 = \frac{1}{r} \tag{85}$$

or, as is well known, the propagation in the numerical lattice along the $\theta_0 = 45^\circ$ line has the minimal anisotropy error (from (85) and (64), $\tan\theta_0 = r\tan\phi_0 = 1$).

Case (2): $P_{\phi 1} = (\Omega_1 \neq 0, K_1, \phi_1)$

Here and in most cases introduced next, we prefer using the polar formulation. Examining (71) one can survey different SOoA_ϕ options leading to different schemes. The two schemes $\mathrm{SOoA}_{\phi 1} = (1,1,3)\ \&\ (1,2,2)$ are readily recognized as unfeasible because (71) yields $c_1^x = c_1^y = 0$ for both cases. The remaining cases are detailed in Appendix C.

6. Two-dimensional examples

6.1. Example: application of the (3,3,0,0) stencils of Section 5.3 to the case $\Delta y = \Delta x$

This case coincides with several schemes available in the literature, that can be used to validate the methodology described herein. Apply $r = 1$ to (62a), i.e. $\gamma_x = \gamma_y = \gamma$

$$\left.\begin{aligned} K_x &= K\cos\phi \\ K_y &= K\sin\phi \end{aligned}\right\} \Rightarrow K^2 = K_x^2 + K_y^2 \tag{86}$$

thereby replacing Eqs. (63) and (64), respectively, with

$$\Omega^2 = \gamma^2(K_x^2 + K_y^2) = \gamma^2 K^2, \tag{87a}$$

$$\frac{K_y}{K_x} = \tan\phi \tag{87b}$$

implying that the direction of propagation in the physical and grid coordinates are the same. For the sake of comparison with existing schemes, we also restrict our discussion to the case $c_1^x = c_1^y = c_1$.

Anisotropy analysis:

Under the aforementioned conditions, the GDE (77) reduces to

$$\cos\Omega = -(c_0 + c_1[\cos(K\cos\phi) + \cos(K\sin\phi)]) \tag{88}$$

such that (85) becomes $\tan\phi_0 = 1 \Rightarrow \phi_0 = \frac{\pi}{4}$. The GDE (88) has a $\frac{\pi}{2}$ periodicity in ϕ in addition to the symmetry mentioned after (77), as duly represented in Fig. 8. Coupled with a proper choice of the zeros of ΔK (see (78)), the periodicity is instrumental in developing schemes that minimize anisotropy errors. Therefore, it would be our goal to preserve this symmetry in other stencil structures with $r = 1$. This may be achieved by imposing conditions on the cs of the GDEs (such as $c_1^x = c_1^y = c_1$).

6.1.1. Examples: categorization of existing (3,3,0,0) schemes

At this point we refer to existing schemes that can be categorized as a subset of the (3,3) stencil with $r = 1$ and $c_1^x = c_1^y = c_1$ and thereby serve as examples, as follows:

(a) $T = 1, P_1 = (0,0,0), \mathrm{SOoA}_1 = (4,4,4)$: standard (2,2) scheme:
Substituting the appropriate values into Eq. (80) results in: $c_1 = -\gamma^2, c_0 = 2\gamma^2 - 1$, that are the coefficients of the standard Yee, S-O [3,3; 2,2] scheme.

(b) $T = 2, P_1 = (0,0,0), P_2 = (\Omega_0, K_0, \phi_0), \mathrm{SOoA}_{\phi 1} = (2,2,2), \mathrm{SOoA}_{\phi 2} = (1,1,1)$:
Subject to the choice of ϕ_0, one can show that this case coincides with the following available schemes: (1) the NSFDTD method [15,16] (originally applied to an extended stencil – see Section 6.2) as applied to the (3,3,0,0) stencil in [19] and (2) schemes in [18] and the INS22 [19]. To this end, apply the GDE (88) at P_1, P_2 and their respective orders $\mathrm{SOoA}_{\phi 1,2}$,

$$1 + c_0 + 2c_1 = 0, \tag{89a}$$

$$\cos\Omega_0 + c_0 + c_1[\cos(K_0\cos\phi_0) + \cos(K_0\sin\phi_0)] = 0 \tag{89b}$$

obtaining the coefficients

$$c_0 = \frac{2\cos\Omega_0 - \cos(K_0\cos\phi_0) - \cos(K_0\sin\phi_0)}{\cos(K_0\cos\phi_0) + \cos(K_0\sin\phi_0) - 2}, \tag{90a}$$

$$c_1 = \frac{1 - \cos\Omega_0}{\cos(K_0\cos\phi_0) + \cos(K_0\sin\phi_0) - 2}. \tag{90b}$$

One can readily see that the choice $\phi_0 = 0$ produces an application of [15,16] to the (3,3,0,0) stencil while $\phi_0 = 22.5^\circ$ reproduces the results found in [18,19].

6.2. Examples: categorization of existing schemes with extended stencils

Our methodology can be viewed in part as a generalization of schemes as in the following examples. These schemes are based on three extended spatial stencils ($(3, 2M+1, D_4, D_8)$ with $M > 1$ and/or $D_4, D_8 > 0$) stencils. The first stencil (Section 6.2.1) supports Cole's NSFDTD scheme [15] that makes use of a nine point stencil, as depicted in Fig. 7(c). In our classification, this stencil is denoted as (3,3,1,0), and is also common to [16,35–37]. Two additional types of schemes (Sections 6.2.3 and 6.2.4), have originated from Maxwell's Equations FDTD (ME-FDTD) and are translated into the equivalent WE-FDTD stencils in this context. In Section 6.2.3, the ME (2,4) stencil [5,7,19,21,23,29,30,32] is translated into the WE-FDTD (3,7,0,0) stencil, giving rise to the type of schemes cited in Section 6.2.3. Next, Section 6.2.4 cites a type of schemes based on the extended (2,6) ME stencil, i.e. [21,24,31,33,34], that is translated into the 21-point (3,5,1,1) WE stencil (see Fig. 7(e)).

6.2.1. Example: (3,3,1,0) stencil based schemes

The stencil structure (3,3,1,0) is shown in Fig. 7(c). Consider the case $\Delta y = \Delta x$, i.e. $r = 1$, therefore K_x and K_y are taken from Eq. (86). The GDE for the (3,3,1,0) stencil, under the symmetry conditions discussed after (88), is

$$\cos\Omega + c_0 + c_1(\cos K_x + \cos K_y) + c_1^d\left[\cos(K_x + K_y) + \cos(K_x - K_y)\right] = 0. \tag{91}$$

Take a single frequency ($T = 1$) at the origin of the dispersion surface. Expand (91) about $P_{\phi 1} = (\Omega_1, K_1, \phi_q) = (0, 0, \phi_q)$ to obtain the following equation in polar coordinates:

$$F(\Omega, K, \phi) = 1 + c_0 + 2(c_1 + c_1^d) - \frac{1}{2}\left[\Omega^2 + K^2\{c_1 + 2c_1^d\}\right] + \frac{1}{24}\left[\Omega^4 + K^4\left\{(c_1 + 2c_1^d)\left(\cos^4\phi_q + \sin^4\phi_q\right) + 12c_1^d\cos^2\phi_q\sin^2\phi_q\right\}\right] + \mathcal{O}\left(\Omega^6 + K^6 + \phi^6\right) = 0. \tag{92}$$

We now have three undetermined coefficient, i.e. c_0, c_1, c_1^d that are required to satisfy the system

$$1 + c_0 + 2(c_1 + c_1^d) = 0, \tag{93a}$$

$$c_1 + 2c_1^d = -\gamma^2, \tag{93b}$$

$$(c_1 + 2c_1^d)\left(\cos^4\phi_q + \sin^4\phi_q\right) + 12c_q^d\cos^2\phi_q\sin^2\phi_q = -\gamma^4 \tag{93c}$$

that arises from (92). It becomes apparent that only one angle can be specified, i.e. $q = 1$. At this angle, we achieve SOoA = (6,6,6) at the origin, hence the designation $\mathrm{SOoA}_{\phi 1} = (6,6,6)|_{\phi_1}$. Suppose we choose $\phi_1 = \frac{\pi}{8}$, then, due to the aforementioned symmetry conditions, the isotropy is also improved at $\frac{\pi}{2} \pm \phi, \pi \pm \phi, \frac{3\pi}{2} \pm \phi$ and $-\phi$ (see Fig. 8). At angles other than these, (93c) does not hold therefore we have SOoA = (4,4,6).

These effects are visible in Fig. 9(a)–(b).

6.2.2. The non-standard FDTD [15], categorized as a (3,3,1,0) stencil based scheme and optimized further

In a frequently cited paper [15], the non-standard approach for derivative discretization [14] was applied to the homogeneous wave equation. The scheme of [15] can be presented in terms of this methodology as follows. Note first that the grid satisfies the condition $r = 1$. One option of utilizing the three degrees of freedom in (91) is with $T = 3$, in which case

$$P_1 = (0,0,0), \quad P_2 = (\Omega_2, K_2, \phi_2), \quad P_3 = (\Omega_2, K_2, \phi_3),$$
$$\mathrm{SOoA}_{\phi 1} = (2,2,2), \quad \mathrm{SOoA}_{\phi 2} = \mathrm{SOoA}_{\phi 3} = (1,1,1).$$

Choose now $\phi_2 = 0^\circ$ and $\phi_3 = 0.18203\pi$. The undetermined coefficients are then the solution for the following system of equations:

$$1 + c_0 + 2(c_1 + c_1^d) = 0, \tag{94a}$$

$$\cos\Omega_2 + c_0 + c_1[\cos(K_2\cos\phi_2) + \cos(K_2\sin\phi_2)] + c_1^d[\cos(K_2[\cos\phi_2 + \sin\phi_2]) + \cos(K_2[\cos\phi_2 - \sin\phi_2])] = 0, \tag{94b}$$

$$\cos\Omega_2 + c_0 + c_1[\cos(K_2\cos\phi_3) + \cos(K_2\sin\phi_3)] + c_1^d[\cos(K_2[\cos\phi_3 + \sin\phi_3]) + \cos(K_2[\cos\phi_3 - \sin\phi_3])] = 0 \tag{94c}$$

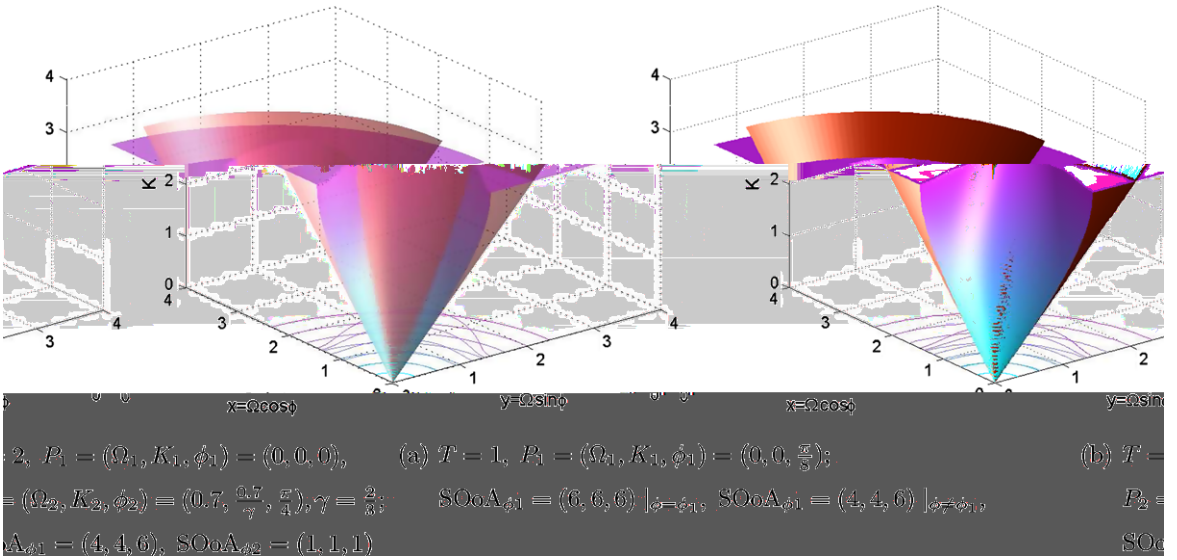

Fig. 9. Two-dimensional dispersion surfaces, Section 6.2.1. Stencil structure vector = (3,3,1,0).

and are related to the parameters u and $\gamma(k,\theta)$ in [15] (not to be confused with the conventional $\gamma = c\frac{\Delta t}{\Delta x}$) by:

$$c_0 = (1+\gamma(k,\theta))\left(\frac{u\Delta t}{\Delta x}\right)^2 - 1, \quad c_1 = -\gamma(k,\theta)\left(\frac{u\Delta t}{\Delta x}\right)^2, \quad c_1^d = -\left(\frac{1-\gamma(k,\theta)}{2}\right)\left(\frac{u\Delta t}{\Delta x}\right)^2.$$

In this way, the non-standard WE-FDTD discretization scheme of [15] can be categorized as an example of this methodology.

This scheme can now be optimized further in terms of isotropy. Analyzing the above mentioned case, it is found that the choice $\phi_2 = 0^\circ$ and $\phi_3 = 0.18203\pi$ made in [15] is not optimal in terms of minimizing the anisotropy error. Our methodology predicts the optimum choice to be $\phi_2 = \frac{\pi}{16}$ and $\phi_3 = \frac{3\pi}{16}$. The improvement In maximum anisotropy error over $0^\circ \leqslant \phi \leqslant 90^\circ$ is demonstrated in Fig. 10.

6.2.3. (3,7,0,0) Stencil WE-FDTD schemes equivalent to (2,4) stencil ME-FDTD schemes

ME-FDTD schemes with (2,4) stencils for both **E** and **H**, where $\Delta x = \Delta y$ and the approximations for both $\frac{\partial}{\partial x}$ and $\frac{\partial}{\partial y}$ are identical, are cited below. These schemes can be translated into equivalent (3,7,0,0) WE stencil schemes with the following form of the GDE:

$$\cos\Omega + c_0 + c_1(\cos K_x + \cos K_y) + c_2(\cos 2K_x + \cos 2K_y) + c_3(\cos 3K_x + \cos 3K_y) = 0. \tag{95}$$

This GDE would be also the result of our WE analysis with (3,7,0,0) stencil with the symmetry conditions specified after (88), i.e. $\Delta x = \Delta y$ and $c_m^x = c_m^y$. The translation from the ME-FDTD results in the following constraints on the coefficients in (95):

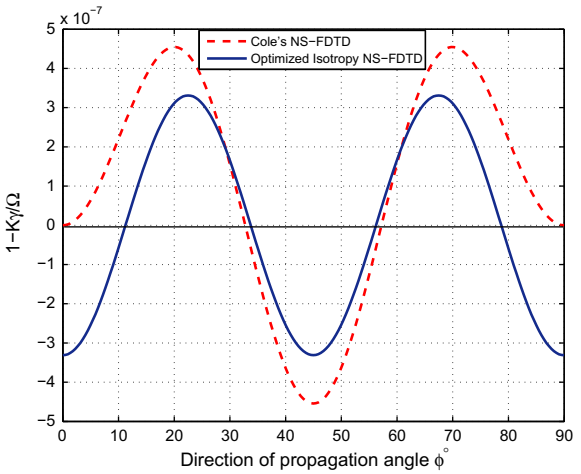

Fig. 10. Anisotropy comparison: $T = 3$: NS-FDTD [15], with $\gamma = \frac{2}{3}, M_{\lambda 2} = M_{\lambda 3} = 8$, samples per wavelength and $\phi_2 = 0, \phi_3 = 0.18203\pi$ vs. optimized Isotropy NS-FDTD with $\phi_2 = \frac{\pi}{16}, \phi_3 = \frac{3\pi}{16}$.

$$(c_2)^2 - 4c_3(c_1 + c_2) = 0, \tag{96a}$$
$$1 + c_0 + 2(c_1 + c_2 + c_3) = 0, \tag{96b}$$

where (96b) shows that adherence to Maxwell's equations implies the inclusion of the origin $P_1 = (0,0,0)$ with $\mathrm{SOoA}_{\phi 1} \geqslant (2,2,2)$. This applies to examples (a) and (b) below.

Examples: categorization of schemes in [21,30,23]

(a) $T = 2, P_1 = (0,0,0), P_2 = (\Omega_2, K_2, \phi_2); \mathrm{SOoA}_{\phi 1} = (4,4,4), \mathrm{SOoA}_{\phi 2} = (1,1,1)$

These schemes can be generated by solving (96) augmented with (97):

$$c_1 + 4c_2 + 9c_3 = -\gamma^2, \tag{97a}$$
$$\cos\Omega_2 + c_0 + c_1[\cos(K_2\cos\phi_2) + \cos(K_2\sin\phi_2)] + c_2[\cos(2K_2\cos\phi_2) + \cos(2K_2\sin\phi_2)] + c_3[\cos(3K_2\cos\phi_2) + \cos(3K_2\sin\phi_2)] = 0. \tag{97b}$$

The first example in this category is the FD24-1 scheme [21]. One can note that Eq. (2) thereof coincides with (97a), establishing the scheme's 2nd OoA ($\mathrm{SOoA}_{\phi 1} = (4,4,4)$ in our designation). The method by which C_2 is found in [21], i.e. a least square optimization carried out on the dispersion relation can be shown to be equivalent to the choice of $\phi_2 = 22.5^\circ$ in (97b). Eqs. (96) and (97) are also equivalent to the scheme in [30] described under the section "a more wideband (2,4) FDTD method".

Two further examples are the Axes Optimized Method (AOM) and the Diagonally Optimized Method (DOM), described in [23]. These two schemes can be shown to coincide with our methodology upon substituting $\phi_2 = 0^\circ$ and $\phi_2 = 45^\circ$, respectively, into (97b).

(b) $T = 3, P_1 = (0,0,0) P_2 = (\Omega_2, K_2, \phi_2), P_3 = (\Omega_2, K_2, \phi_3); \mathrm{SOoA}_{\phi 1} = (2,2,2), \mathrm{SOoA}_{\phi 2} = \mathrm{SOoA}_{\phi 3} = (1,1,1)$

The "fully optimized" and FD24-2 schemes of [30,21], respectively, trade second OoA for better isotropy at a given frequency. In [21], this is done by modifying Eq. (2) into (3) with the addition of another degree of freedom denoted p, in addition to C_2, and again performing the least square minimization of the anisotropy error over the angular space. This scheme can be shown to be equivalent to a the scheme resulting from our methodology (97) replaced by (98):

$$\cos\Omega_2 + c_0 + c_1[\cos(K_2\cos\phi_2) + \cos(K_2\sin\phi_2)] + c_2[\cos(2K_2\cos\phi_2) + \cos(2K_2\sin\phi_2)] + c_3[\cos(3K_2\cos\phi_2) + \cos(3K_2\sin\phi_2)] = 0, \tag{98a}$$
$$\cos\Omega_2 + c_0 + c_1[\cos(K_2\cos\phi_3) + \cos(K_2\sin\phi_3)] + c_2[\cos(2K_2\cos\phi_3) + \cos(2K_2\sin\phi_3)] + c_3[\cos(3K_2\cos\phi_3) + \cos(3K_2\sin\phi_3)] = 0 \tag{98b}$$

using $\phi_2 = 11.25^\circ$ and $\phi_3 = 33.75^\circ$.

The choice $\phi_2 = 0^\circ$ and $\phi_3 = 45^\circ$ in (98) can also be shown equivalent to the "modified operator schemes" and Isotropic Optimization Method (IOM) of [30] and [23], respectively.

6.2.4. (3,5,1,1) Stencil WE-FDTD schemes equivalent to diagonally extended (2,6) stencil ME-FDTD schemes

ME-FDTD schemes based on diagonally extended (2,6) stencils are translatable to WE schemes with stencil size (3,5,1,1). Imposing the same conditions as specified in Section 6.2.3 before (96), the GDE schemes based on this stencil are

$$\cos\Omega + c_0 + c_1(\cos K_x + \cos K_y) + c_1^d[\cos(K_x - K_y) + \cos(K_x + K_y)] + c_2\left\{\cos 2K_x + \cos 2K_y - \frac{1}{2}\left[\cos(K_x + 2K_y) + \cos(K_x - 2K_y) + \cos(2K_x + K_y) + \cos(2K_x - K_y)\right]\right\} = 0. \tag{99}$$

Similarly, the equations corresponding to (96) are

$$(c_1^d)^2 + 8c_2(c_1 + c_2 + c_1^d) = 0, \tag{100a}$$
$$1 + c_0 + 2(c_1 + c_1^d) = 0. \tag{100b}$$

Examples: categorization of further schemes in [21,24,33]

(a) $T = 2, P_1 = (0,0,0), P_2 = (\Omega_2, K_2, \phi_2); \mathrm{SOoA}_{\phi 1} = (4,4,4), \mathrm{SOoA}_{\phi 2} = (1,1,1)$

The scheme denoted FD26-1 in [21] can be generated by augmenting Eq. (100) with

$$c_1 - c_2 + 2c_1^d = -\gamma^2, \tag{101a}$$
$$\cos\Omega_2 + c_0 + c_1[\cos(K_2\cos\phi_2) + \cos(K_2\sin\phi_2)] + 2c_1^d\cos(K_2\cos\phi_2)\cos(K_2\sin\phi_2) + 2c_2\left[\cos(2K_2\cos\phi_2)\sin^2\frac{K_2\sin\phi_2}{2} + \cos(2K_2\sin\phi_2)\sin^2\frac{K_2\cos\phi_2}{2}\right] = 0, \tag{101b}$$

where (101a) is the second order term of (99) at P_1 while (101b) is the zeroth order of the polar representation of (99) at P_2 with $\phi_2 = 30^\circ$.

(b) $T = 3, P_1 = (0,0,0), P_2 = (\Omega_2, K_2, \phi_2), P_3 = (\Omega_2, K_2, \phi_3); \mathrm{SOoA}_{\phi 1} = (2,2,2), \mathrm{SOoA}_{\phi 2} = \mathrm{SOoA}_{\phi 3} = (1,1,1)$

The following available schemes can be categorized under this type of WE schemes. Augment (100) with (101b) applied twice, with P_2 and P_3. The Neighborhood Averaging (NA) scheme of [24] is the outcome of substituting $\phi_2 = 0^\circ$

and $\phi_3 = 45^\circ$ into these two equations. The FD26-2 of [21] is reproduced by choosing $\phi_2 = 11.25^\circ$ and $\phi_3 = 33.75^\circ$. Similarly, the scheme in [33] emerges upon choosing $\phi_2 = 0^\circ$ and ϕ_3 that is the angle corresponding to a given α in [33].

7. Conclusions

The methodology for constructing stable WE-FDTD schemes for given $(3, 2M+1)$ 1-D and $(3,3)$ 2-D stencils, tailored to the spectral property of the excitation, has been developed and demonstrated. The generalized dispersion equation (GDE) with undetermined coefficients is made to fit the linear dispersion curve/surface at arbitrary spectral point Ω_q, K_q to a certain SOoA using a Taylor expansion about that point. The SOoA concept includes phase and group dispersion control as special cases. Unlike many available schemes, strict OoA behavior is not considered crucial for electromagnetic high frequency pulses. The available degrees of freedom can thus be used to enhance accuracy at higher frequencies, possibly at the expense of low frequency behavior. As a result, simulations with about one million time steps have been demonstrated.

This work was performed mainly in the context of the wave equation. Two- dimensional examples in Section 6.2 that have been originally developed for Maxwell's equations have been translated to the wave equation case based on this work. For the one-dimensional Maxwell's equations case, the equivalent of the GDE (5) is a general spectral Maxwell's equations

$$E_0 \sin\left(\frac{\Omega}{2}\right) = -\eta\left[\sum_{m=1}^{M} b_{hm} \sin\left(\frac{(2m-1)K}{2}\right)\right] H_0, \tag{102a}$$

$$H_0 \sin\left(\frac{\Omega}{2}\right) = -\frac{1}{\eta}\left[\sum_{m=1}^{M} b_{em} \sin\left(\frac{(2m-1)K}{2}\right)\right] E_0, \tag{102b}$$

where η is the wave impedance. Using an analogous rationale to this work, the counterpart of (5) can be derived, and relationships to the wave equation formulations deduced.

The methodology developed here is seen as a generalization of existing schemes. The two-dimensional examples cited on Sections 6.1 and 6.2 serve in effect to validate the formulation in Section 5. It should be noted that for the two-dimensional case, the polar formulation is generally preferred for reasons outlined after Eq. (69).

Acknowledgment

This work was supported in part by the Israel Science Foundation (ISF) under grant 1237/06.

Appendix A. Details of the one-dimensional cases for the (3,5) stencil with $T = 2$ and $T = 3$

This appendix augments the case $T = 1$ given in Section 3.2.1.

A.1. $T = 2$

The cases $(\Omega_2, K_2) > (\Omega_1, K_1) = (0,0)$:

(a) $\mathrm{SOoA}_1 = (2,4), \mathrm{SOoA}_2 = (1,1)$ (b) $\mathrm{SOoA}_1 = (4,4), \mathrm{SOoA}_2 = (1,1)$ (c) $\mathrm{SOoA}_1 = (2,2), \mathrm{SOoA}_2 = (1,2)$ (d) $\mathrm{SOoA}_1 = (2,2), \mathrm{SOoA}_2 = (2,2)$

Eq. (18) becomes, for the respective SOoAs,

$$\begin{pmatrix} 1 & 1 & 1 \\ 0 & 1 & 1 \\ 1 & \cos K_2 & \cos 2K_2 \end{pmatrix} * \begin{pmatrix} 1 & 1 & 1 \\ 0 & 1^2 & 2^2 \\ 1 & 1 & 1 \end{pmatrix} \cdot \begin{pmatrix} c_0 \\ c_1 \\ c_2 \end{pmatrix} = \begin{pmatrix} 1 \\ 1 \\ \cos\Omega_2 \end{pmatrix} * \underbrace{\begin{pmatrix} -1 \\ 0 \\ -1 \end{pmatrix}}_{(a)} ; \underbrace{\begin{pmatrix} -1 \\ -\gamma^2 \\ -1 \end{pmatrix}}_{(b)}, \tag{103}$$

$$\begin{pmatrix} 1 & 1 & 1 \\ 1 & \cos K_2 & \cos 2K_2 \\ 0 & \sin K_2 & \sin 2K_2 \end{pmatrix} * \begin{pmatrix} 1 & 1 & 1 \\ 1 & 1 & 1 \\ 0 & 1 & 2 \end{pmatrix} \cdot \begin{pmatrix} c_0 \\ c_1 \\ c_2 \end{pmatrix} = \begin{pmatrix} 1 \\ \cos\Omega_2 \\ \sin\Omega_2 \end{pmatrix} * \underbrace{\begin{pmatrix} -1 \\ -1 \\ 0 \end{pmatrix}}_{(c)} ; \underbrace{\begin{pmatrix} -1 \\ -1 \\ -\gamma \end{pmatrix}}_{(d)}. \tag{104}$$

The cases $(\Omega_2, K_2) > (\Omega_1, K_1) > (0,0)$:

(e) $\mathrm{SOoA}_1 = (1,1), \mathrm{SOoA}_2 = (1,2)$ (f) $\mathrm{SOoA}_1 = (1,1), \mathrm{SOoA}_2 = (2,2)$ (18) becomes, for the respective SOoAs,

$$\begin{pmatrix} 1 & \cos K_1 & \cos 2K_1 \\ 1 & \cos K_2 & \cos 2K_2 \\ 0 & \sin K_2 & \sin 2K_2 \end{pmatrix} * \begin{pmatrix} 1 & 1 & 1 \\ 1 & 1 & 1 \\ 0 & 1 & 2 \end{pmatrix} \cdot \begin{pmatrix} c_0 \\ c_1 \\ c_2 \end{pmatrix} = \begin{pmatrix} \cos\Omega_1 \\ \cos\Omega_2 \\ \sin\Omega_2 \end{pmatrix} * \underbrace{\begin{pmatrix} -1 \\ -1 \\ 0 \end{pmatrix}}_{(a)} ; \underbrace{\begin{pmatrix} -1 \\ -1 \\ -\gamma \end{pmatrix}}_{(b)}. \tag{105}$$

The companion cases
(e′) $\mathrm{SOoA}_1 = (1,2), \mathrm{SOoA}_2 = (1,1)$ (f′) $\mathrm{SOoA}_1 = (2,2), \mathrm{SOoA}_2 = (1,1)$
that incorporate permutations of the same equations, are similarly derived. For cases (a), (c) and (e′), stability regions have not been found. Cases (b), (d) and (f′) have stability regions as shown in Fig. 3(a)–(c), respectively.

A.2. $T = 3$

(a) $(\Omega_3, K_3) > (\Omega_2, K_2) > (\Omega_1, K_1) = (0,0), \mathrm{SOoA}_1 = (2,2), \mathrm{SOoA}_2 = \mathrm{SOoA}_3 = (1,1)$

$$\begin{pmatrix} 1 & 1 & 1 \\ 1 & \cos K_2 & \cos 2K_2 \\ 1 & \cos K_3 & \cos 2K_3 \end{pmatrix} * \begin{pmatrix} 1 & 1 & 1 \\ 1 & 1 & 1 \\ 1 & 1 & 1 \end{pmatrix} \cdot \begin{pmatrix} c_0 \\ c_1 \\ c_2 \end{pmatrix} = \begin{pmatrix} 1 \\ \cos\Omega_2 \\ \cos\Omega_3 \end{pmatrix} * \underbrace{\begin{pmatrix} -1 \\ -1 \\ -1 \end{pmatrix}}_{(a)}. \tag{106}$$

(b) $(\Omega_3, K_3) > (\Omega_2, K_2) > (\Omega_1, K_1) > (0,0), \mathrm{SOoA}_1 = \mathrm{SOoA}_2 = \mathrm{SOoA}_3 = (1,1)$

$$\begin{pmatrix} 1 & \cos K_1 & \cos 2K_1 \\ 1 & \cos K_2 & \cos 2K_2 \\ 1 & \cos K_3 & \cos 2K_3 \end{pmatrix} * \begin{pmatrix} 1 & 1 & 1 \\ 1 & 1 & 1 \\ 1 & 1 & 1 \end{pmatrix} \cdot \begin{pmatrix} c_0 \\ c_1 \\ c_2 \end{pmatrix} = \begin{pmatrix} \cos\Omega_1 \\ \cos\Omega_2 \\ \cos\Omega_3 \end{pmatrix} * \underbrace{\begin{pmatrix} -1 \\ -1 \\ -1 \end{pmatrix}}_{(b)}. \tag{107}$$

These two cases have stability regions shown in Fig. 3(d) and (e), respectively. Again, the schemes for $T = 2$ and $T = 3$ do not seem to have documented counterparts.

Appendix B. Details of the one-dimensional cases for the (3,7) stencil with $T = 2$ through $T = 4$

This appendix augments the case $T = 1$ of Section 3.3.1.

B.1. $T = 2$

The cases $(\Omega_2, K_2) > (\Omega_1, K_1) = (0,0)$:
(a) $\mathrm{SOoA}_1 = (2,6), \mathrm{SOoA}_2 = (1,1)$ (b) $\mathrm{SOoA}_1 = (4,6), \mathrm{SOoA}_2 = (1,1)$ (c) $\mathrm{SOoA}_1 = (6,6), \mathrm{SOoA}_2 = (1,1)$

$$\begin{pmatrix} 1 & 1 & 1 & 1 \\ 0 & 1 & 1 & 1 \\ 0 & 1 & 1 & 1 \\ 1 & \cos K_2 & \cos 2K_2 & \cos 3K_2 \end{pmatrix} * \begin{pmatrix} 1 & 1 & 1 & 1 \\ 0 & 1^2 & 2^2 & 3^2 \\ 0 & 1^4 & 2^4 & 3^4 \\ 1 & 1 & 1 & 1 \end{pmatrix} \cdot \begin{pmatrix} c_0 \\ c_1 \\ c_2 \\ c_3 \end{pmatrix} = \begin{pmatrix} 1 \\ 1 \\ 1 \\ \cos\Omega_2 \end{pmatrix} * \underbrace{\begin{pmatrix} -1 \\ 0 \\ 0 \\ -1 \end{pmatrix}}_{(a)}; \underbrace{\begin{pmatrix} -1 \\ -\gamma^2 \\ 0 \\ -1 \end{pmatrix}}_{(b)}; \underbrace{\begin{pmatrix} -1 \\ -\gamma^2 \\ -\gamma^4 \\ -1 \end{pmatrix}}_{(c)}. \tag{108}$$

For case (a) the S-O is undefined. For cases (b) and (c), the S-Os are [3,7; 2,4] and [3,7; 4,4], respectively.
The cases $(\Omega_2, K_2) > (\Omega_1, K_1) = (0,0)$:
(d) $\mathrm{SOoA}_1 = (2,4), \mathrm{SOoA}_2 = (1,2)$ (e) $\mathrm{SOoA}_1 = (2,4), \mathrm{SOoA}_2 = (2,2)$ (f) $\mathrm{SOoA}_1 = (4,4), \mathrm{SOoA}_2 = (1,2)$
(g) $\mathrm{SOoA}_1 = (4,4), \mathrm{SOoA}_2 = (2,2)$

$$\begin{pmatrix} 1 & 1 & 1 & 1 \\ 0 & 1 & 1 & 1 \\ 1 & \cos K_2 & \cos 2K_2 & \cos 3K_2 \\ 0 & \sin K_2 & \sin 2K_2 & \sin 3K_2 \end{pmatrix} * \begin{pmatrix} 1 & 1 & 1 & 1 \\ 0 & 1^2 & 2^2 & 3^2 \\ 1 & 1 & 1 & 1 \\ 0 & 1 & 2 & 3 \end{pmatrix} \cdot \begin{pmatrix} c_0 \\ c_1 \\ c_2 \\ c_3 \end{pmatrix} = \begin{pmatrix} 1 \\ 1 \\ \cos\Omega_2 \\ \sin\Omega_2 \end{pmatrix} * \underbrace{\begin{pmatrix} -1 \\ 0 \\ -1 \\ 0 \end{pmatrix}}_{(d)}; \underbrace{\begin{pmatrix} -1 \\ 0 \\ -1 \\ -\gamma \end{pmatrix}}_{(e)}; \underbrace{\begin{pmatrix} -1 \\ -\gamma^2 \\ -1 \\ 0 \end{pmatrix}}_{(f)}; \underbrace{\begin{pmatrix} -1 \\ -\gamma^2 \\ -1 \\ -\gamma \end{pmatrix}}_{(g)}. \tag{109}$$

The cases $(\Omega_2, K_2) > (\Omega_1, K_1) = (0,0)$:
(h) $\mathrm{SOoA}_1 = (2,2), \mathrm{SOoA}_2 = (1,3)$ (i) $\mathrm{SOoA}_1 = (2,2), \mathrm{SOoA}_2 = (2,3)$ (j) $\mathrm{SOoA}_1 = (2,2), \mathrm{SOoA}_2 = (3,3)$

$$\begin{pmatrix} 1 & 1 & 1 & 1 \\ 1 & \cos K_2 & \cos 2K_2 & \cos 3K_2 \\ 0 & \sin K_2 & \sin 2K_2 & \sin 3K_2 \\ 0 & \cos K_2 & \cos 2K_2 & \cos 3K_2 \end{pmatrix} * \begin{pmatrix} 1 & 1 & 1 & 1 \\ 1 & 1 & 1 & 1 \\ 0 & 1 & 2 & 3 \\ 0 & 1^2 & 2^2 & 3^2 \end{pmatrix} \cdot \begin{pmatrix} c_0 \\ c_1 \\ c_2 \\ c_3 \end{pmatrix} = \begin{pmatrix} 1 \\ \cos\Omega_2 \\ \sin\Omega_2 \\ \cos\Omega_2 \end{pmatrix} * \underbrace{\begin{pmatrix} -1 \\ -1 \\ 0 \\ 0 \end{pmatrix}}_{(h)}; \underbrace{\begin{pmatrix} -1 \\ -1 \\ -\gamma \\ 0 \end{pmatrix}}_{(i)}; \underbrace{\begin{pmatrix} -1 \\ -1 \\ -\gamma \\ -\gamma^2 \end{pmatrix}}_{(j)}. \tag{110}$$

Table B.1
Existence of stability regions for the (3,7) stencil schemes: ✓ = existing, X = not found.

Scheme	Stability regions
3.3.1 : $T = 1$	
(a)	✓
(b)	✓
(c)	✓
(d)	X
(e)	X
(f)	X

Scheme	Stability regions
3.3.2 : $T = 2$	
(a)	✓
(b)	✓
(c)	✓
(d)	X
(e)	X
(f)	X
(g)	✓
(j)	✓
(k)	✓
(l)	X
(m)	X
(n)	X
(o)	X
(p)	X

Scheme	Stability regions
3.3.3 : $T = 3$	
(a)	X
(b)	✓
(c)	X
(d)	✓
(e)	X
(f)	X
3.3.4 : $T = 4$	
(a)	✓
(b)	X

The cases $(\Omega_2, K_2) > (\Omega_1, K_1) > (0,0)$:
(k) $\mathrm{SOoA}_1 = (1,3), \mathrm{SOoA}_2 = (1,1)$ (l) $\mathrm{SOoA}_1 = (2,3), \mathrm{SOoA}_2 = (1,1)$ (m) $\mathrm{SOoA}_1 = (3,3), \mathrm{SOoA}_2 = (1,1)$

$$\begin{pmatrix} 1 & \cos K_1 & \cos 2K_1 & \cos 3K_1 \\ 0 & \sin K_1 & \sin 2K_1 & \sin 3K_1 \\ 0 & \cos K_1 & \cos 2K_1 & \cos 3K_1 \\ 1 & \cos K_2 & \cos 2K_2 & \cos 3K_2 \end{pmatrix} * \begin{pmatrix} 1 & 1 & 1 & 1 \\ 0 & 1 & 2 & 3 \\ 0 & 1^2 & 2^2 & 3^2 \\ 1 & 1 & 1 & 1 \end{pmatrix} \cdot \begin{pmatrix} c_0 \\ c_1 \\ c_2 \\ c_3 \end{pmatrix} = \begin{pmatrix} \cos \Omega_1 \\ \sin \Omega_1 \\ \cos \Omega_1 \\ \cos \Omega_2 \end{pmatrix} * \underbrace{\begin{pmatrix} -1 \\ 0 \\ 0 \\ -1 \end{pmatrix}}_{(k)}; \underbrace{\begin{pmatrix} -1 \\ -\gamma \\ 0 \\ -1 \end{pmatrix}}_{(l)}; \underbrace{\begin{pmatrix} -1 \\ -\gamma \\ -\gamma^2 \\ -1 \end{pmatrix}}_{(m)}. \tag{111}$$

The cases $(\Omega_2, K_2) > (\Omega_1, K_1) > (0,0)$:
(n) $\mathrm{SOoA}_1 = (1,2), \mathrm{SOoA}_2 = (1,2)$ (o) $\mathrm{SOoA}_1 = (1,2), \mathrm{SOoA}_2 = (2,2)$ (p) $\mathrm{SOoA}_1 = (2,2), \mathrm{SOoA}_2 = (2,2)$

$$\begin{pmatrix} 1 & \cos K_1 & \cos 2K_1 & \cos 3K_1 \\ 0 & \sin K_1 & \sin 2K_1 & \sin 3K_1 \\ 1 & \cos K_2 & \cos 2K_2 & \cos 3K_2 \\ 0 & \sin K_2 & \sin 2K_2 & \sin 3K_2 \end{pmatrix} * \begin{pmatrix} 1 & 1 & 1 & 1 \\ 0 & 1 & 2 & 3 \\ 1 & 1 & 1 & 1 \\ 0 & 1 & 2 & 3 \end{pmatrix} \cdot \begin{pmatrix} c_0 \\ c_1 \\ c_2 \\ c_3 \end{pmatrix} = \begin{pmatrix} \cos \Omega_1 \\ \sin \Omega_1 \\ \cos \Omega_2 \\ \sin \Omega_2 \end{pmatrix} * \underbrace{\begin{pmatrix} -1 \\ 0 \\ -1 \\ 0 \end{pmatrix}}_{(n)}; \underbrace{\begin{pmatrix} -1 \\ 0 \\ -1 \\ -\gamma \end{pmatrix}}_{(o)}; \underbrace{\begin{pmatrix} -1 \\ -\gamma \\ -1 \\ -\gamma \end{pmatrix}}_{(p)}. \tag{112}$$

The companion cases
(k′) $\mathrm{SOoA}_1 = (1,1), \mathrm{SOoA}_2 = (1,3)$ (l′) $\mathrm{SOoA}_1 = (1,1), \mathrm{SOoA}_2 = (2,3)$ (m′) $\mathrm{SOoA}_1 = (1,1), \mathrm{SOoA}_2 = (3,3)$ (o′) $\mathrm{SOoA}_1 = (2,2), \mathrm{SOoA}_2 = (1,2)$
that incorporate permutations of the same equations, are similarly derived.

B.2. $T = 3$

The cases $(\Omega_3, K_3) > (\Omega_2, K_2) > (\Omega_1, K_1) = (0,0)$:
(a) $\mathrm{SOoA}_1 = (2,4), \mathrm{SOoA}_{2,3} = (1,1)$ (b) $\mathrm{SOoA}_1 = (4,4), \mathrm{SOoA}_{2,3} = (1,1)$

$$\begin{pmatrix} 1 & 1 & 1 & 1 \\ 0 & 1 & 1 & 1 \\ 1 & \cos K_2 & \cos 2K_2 & \cos 3K_2 \\ 1 & \cos K_3 & \cos 2K_3 & \cos 3K_3 \end{pmatrix} * \begin{pmatrix} 1 & 1 & 1 & 1 \\ 0 & 1^2 & 2^2 & 3^2 \\ 1 & 1 & 1 & 1 \\ 1 & 1 & 1 & 1 \end{pmatrix} \cdot \begin{pmatrix} c_0 \\ c_1 \\ c_2 \\ c_3 \end{pmatrix} = \begin{pmatrix} 1 \\ 1 \\ \cos \Omega_2 \\ \cos \Omega_3 \end{pmatrix} * \underbrace{\begin{pmatrix} -1 \\ 0 \\ -1 \\ -1 \end{pmatrix}}_{(a)} ; \underbrace{\begin{pmatrix} -1 \\ -\gamma^2 \\ -1 \\ -1 \end{pmatrix}}_{(b)} . \tag{113}$$

The cases $(\Omega_3, K_3) > (\Omega_2, K_2) > (\Omega_1, K_1) = (0,0)$:
(c) $\mathrm{SOoA}_1 = (2,2), \mathrm{SOoA}_2 = (1,2), \mathrm{SOoA}_3 = (1,1)$ (d) $\mathrm{SOoA}_{1,2} = (2,2), \mathrm{SOoA}_3 = (1,1)$

$$\begin{pmatrix} 1 & 1 & 1 & 1 \\ 1 & \cos K_2 & \cos 2K_2 & \cos 3K_2 \\ 0 & \sin K_2 & \sin 2K_2 & \sin 3K_2 \\ 1 & \cos K_3 & \cos 2K_3 & \cos 3K_3 \end{pmatrix} * \begin{pmatrix} 1 & 1 & 1 & 1 \\ 1 & 1 & 1 & 1 \\ 0 & 1 & 2 & 3 \\ 1 & 1 & 1 & 1 \end{pmatrix} \cdot \begin{pmatrix} c_0 \\ c_1 \\ c_2 \\ c_3 \end{pmatrix} = \begin{pmatrix} 1 \\ \cos \Omega_2 \\ \sin \Omega_2 \\ \cos \Omega_3 \end{pmatrix} * \underbrace{\begin{pmatrix} -1 \\ -1 \\ 0 \\ -1 \end{pmatrix}}_{(c)} ; \underbrace{\begin{pmatrix} -1 \\ -1 \\ -\gamma \\ -1 \end{pmatrix}}_{(d)} . \tag{114}$$

The cases $(\Omega_3, K_3) > (\Omega_2, K_2) > (\Omega_1, K_1) > (0,0)$:
(e) $\mathrm{SOoA}_1 = (1,2), \mathrm{SOoA}_{2,3} = (1,1)$ (f) $\mathrm{SOoA}_1 = (2,2), \mathrm{SOoA}_{2,3} = (1,1)$

$$\begin{pmatrix} 1 & \cos K_1 & \cos 2K_1 & \cos 3K_1 \\ 0 & \sin K_1 & \sin 2K_1 & \sin 3K_1 \\ 1 & \cos K_2 & \cos 2K_2 & \cos 3K_2 \\ 1 & \cos K_3 & \cos 2K_3 & \cos 3K_3 \end{pmatrix} * \begin{pmatrix} 1 & 1 & 1 & 1 \\ 0 & 1 & 2 & 3 \\ 1 & 1 & 1 & 1 \\ 1 & 1 & 1 & 1 \end{pmatrix} \cdot \begin{pmatrix} c_0 \\ c_1 \\ c_2 \\ c_3 \end{pmatrix} = \begin{pmatrix} \cos \Omega_1 \\ \sin \Omega_1 \\ \cos \Omega_2 \\ \cos \Omega_3 \end{pmatrix} * \underbrace{\begin{pmatrix} -1 \\ 0 \\ -1 \\ -1 \end{pmatrix}}_{(e)} ; \underbrace{\begin{pmatrix} -1 \\ -\gamma \\ -1 \\ -1 \end{pmatrix}}_{(f)} . \tag{115}$$

Companion cases, of the type mentioned after (112), are also derivable.

B.3. $T = 4$

(a) $(\Omega_4, K_4) > (\Omega_3, K_3) > (\Omega_2, K_2) > (\Omega_1, K_1) = (0,0)$, $\mathrm{SOoA}_1 = (2,2), \mathrm{SOoA}_{2,3,4} = (1,1)$:

$$\begin{pmatrix} 1 & 1 & 1 & 1 \\ 1 & \cos K_2 & \cos 2K_2 & \cos 3K_2 \\ 1 & \cos K_3 & \cos 2K_3 & \cos 3K_3 \\ 1 & \cos K_4 & \cos 2K_4 & \cos 3K_4 \end{pmatrix} * \begin{pmatrix} 1 & 1 & 1 & 1 \\ 1 & 1 & 1 & 1 \\ 1 & 1 & 1 & 1 \\ 1 & 1 & 1 & 1 \end{pmatrix} \cdot \begin{pmatrix} c_0 \\ c_1 \\ c_2 \\ c_3 \end{pmatrix} = \begin{pmatrix} 1 \\ \cos \Omega_2 \\ \cos \Omega_3 \\ \cos \Omega_4 \end{pmatrix} * \underbrace{\begin{pmatrix} -1 \\ -1 \\ -1 \\ -1 \end{pmatrix}}_{(a)} . \tag{116}$$

(b) $(\Omega_4, K_4) > (\Omega_3, K_3) > (\Omega_2, K_2) > (\Omega_1, K_1) > (0,0), \mathrm{SOoA}_{1,2,3,4} = (1,1)$:

$$\begin{pmatrix} 1 & \cos K_1 & \cos 2K_1 & \cos 3K_1 \\ 1 & \cos K_2 & \cos 2K_2 & \cos 3K_2 \\ 1 & \cos K_3 & \cos 2K_3 & \cos 3K_3 \\ 1 & \cos K_4 & \cos 2K_4 & \cos 3K_4 \end{pmatrix} * \begin{pmatrix} 1 & 1 & 1 & 1 \\ 1 & 1 & 1 & 1 \\ 1 & 1 & 1 & 1 \\ 1 & 1 & 1 & 1 \end{pmatrix} \cdot \begin{pmatrix} c_0 \\ c_1 \\ c_2 \\ c_3 \end{pmatrix} = \begin{pmatrix} \cos \Omega_1 \\ \cos \Omega_2 \\ \cos \Omega_3 \\ \cos \Omega_4 \end{pmatrix} * \underbrace{\begin{pmatrix} -1 \\ -1 \\ -1 \\ -1 \end{pmatrix}}_{(b)} . \tag{117}$$

Appendix C. Details of two-dimensional cases

This appendix augments the case described in Section 5.3.1.

C.1. T=1

(a) $\mathrm{SOoA}_{\phi 1} = (1,3,1)$
The system of equations resulting from (71) for this case is

$$c_0 + \cos \Omega_1 + c_1^x \cos(K_1 \cos \phi_1) + c_1^y \cos(rK_1 \sin \phi_1) = 0, \tag{118a}$$

$$c_1^x \sin(K_1 \cos \phi_1) \cos \phi_1 + c_1^y \sin(rK_1 \sin \phi_1) r \sin \phi_1 = 0, \tag{118b}$$

$$c_1^x \cos(K_1 \cos \phi_1) \cos^2 \phi_1 + c_1^y \cos(rK_1 \sin \phi_1) r^2 \sin^2 \phi_1 = -\gamma_x^2 \cos \Omega_1 \tag{118c}$$

with the resultant coefficients:

$$\begin{pmatrix} c_1^x \\ c_1^y \end{pmatrix} = \gamma_x^2 \cos\Omega_1 \begin{pmatrix} (\sin(K_1\cos\phi_1)\cos^2\phi_1[\cot(rK_1\sin\phi_1)r\tan\phi_1 - \cot(K_1\cos\phi_1)])^{-1} \\ -2(\sin(rK_1\sin\phi_1)r\sin(2\phi_1)[\cot(rK_1\sin\phi_1)r\tan\phi_1 - \cot(K_1\cos\phi_1)])^{-1} \end{pmatrix},$$

$$c_0; = -\left[\cos\Omega_1 + c_1^x\cos(K_1\cos\phi_1) + c_1^y\cos(rK_1\sin\phi_1)\right].$$

In the cases that follow maintain Eq. (118a) and only specify the two equations replacing (118b) and (118c).

(b) $\mathrm{SOoA}_{\phi 1} = (2,2,2)$
This case is discussed above in conjunction with Eqs. (68) and (69).

(c) $\mathrm{SOoA}_{\phi 1} = (2,3,1)$
For this case, replace the right hand sides of (118b) and (118c) by $-\gamma_x \sin\Omega_1$ and 0, respectively.

(d) $\mathrm{SOoA}_{\phi 1} = (3,3,1)$
Here, replace the R.H.S. of Eq. (118b) with $-\gamma_x \sin\Omega_1$ and leave (118c) unchanged.

C.2. $T = 2$

Cases (a)–(c) below are with $P_{\phi 1} = (0,0,0), P_{\phi 2} = (\Omega_2 \neq 0, K_2, \phi_2)$; cases (d)–(f) have $P_{\phi 1} = (\Omega_1 \neq 0, K_1, \phi_1), P_{\phi 2} = (\Omega_2 \neq 0, K_2, \phi_2)$

(a) $\mathrm{SOoA}_{\phi 1} = (2,2,2), \mathrm{SOoA}_{\phi 2} = (1,1,2)$. Here the appropriate system is:

$$1 + c_0 + c_1^x + c_1^y = 0, \tag{119a}$$

$$\cos\Omega_2 + c_0 + c_1^x\cos(K_2\cos\phi_2) + c_1^y\cos(rK_2\sin\phi_2) = 0, \tag{119b}$$

$$c_1^x\sin(K_2\cos\phi_2)K_2\sin\phi_2 - c_1^y\sin(rK_2\sin\phi_2)rK_2\cos\phi_2 = 0. \tag{119c}$$

(b) $\mathrm{SOoA}_{\phi 1} = (2,2,2), \mathrm{SOoA}_{\phi 2} = (1,2,1)$. This case requires replacing Eq. (119c) with

$$c_1^x\sin(K_2\cos\phi_2)\cos\phi_2 + c_1^y\sin(rK_2\sin\phi_2)r\sin\phi_2 = 0. \tag{120}$$

(c) $\mathrm{SOoA}_{\phi 1} = (2,2,2), \mathrm{SOoA}_{\phi 2} = (2,2,1)$. This case is the result of replacing the 0 in the R.H.S. of Eq. (120) with $-\gamma_x \sin\Omega_2$.
The next schemes (d)–(f) are derivable from cases (a)–(c) above by replacing (119a) with

$$\cos\Omega_1 + c_0 + c_1^x\cos(K_1\cos\phi_1) + c_1^y\cos(rK_1\sin\phi_1) = 0. \tag{121}$$

(d) $\mathrm{SOoA}_{\phi 1} = (1,1,1), \mathrm{SOoA}_{\phi 2} = (1,1,2)$
(e) $\mathrm{SOoA}_{\phi 1} = (1,1,1), \mathrm{SOoA}_{\phi 2} = (1,2,1)$
(f) $\mathrm{SOoA}_{\phi 1} = (1,1,1), \mathrm{SOoA}_{\phi 2} = (2,2,1)$

C.3. $T = 3$

(a) $\mathrm{SOoA}_{\phi 1} = (2,2,2), \mathrm{SOoA}_{\phi 2,3} = (1,1,1)$
Here, $P_{\phi 1} = (0,0,0)$, $P_{\phi 2} = (\Omega_2 \neq 0, K_2, \phi_2)$, $P_{\phi 3} = (\Omega_3 \neq 0, K_3, \phi_3)$. The system of equations defining this case is:

$$1 + c_0 + c_1^x + c_1^y = 0, \tag{122a}$$

$$\cos\Omega_2 + c_0 + c_1^x\cos(K_2\cos\phi_2) + c_1^y\cos(rK_2\sin\phi_2) = 0, \tag{122b}$$

$$\cos\Omega_3 + c_0 + c_1^x\cos(K_3\cos\phi_3) + c_1^y\cos(rK_3\sin\phi_3) = 0. \tag{122c}$$

(b) $\mathrm{SOoA}_{\phi 1} = \mathrm{SOoA}_{\phi 2} = \mathrm{SOoA}_{\phi 3} = (1,1,1)$. With $P_{\phi 1} = (\Omega_1 \neq 0, K_1, \phi_1), P_{\phi 2} = (\Omega_2 \neq 0, K_2, \phi_2)$, $P_{\phi 3} = (\Omega_3 \neq 0, K_3, \phi_3)$. This scheme is the result of replacing Eq. (122a) with:

$$\cos\Omega_1 + c_0 + c_1^x\cos(K_1\cos\phi_1) + c_1^y\cos(rK_1\sin\phi_1) = 0. \tag{123}$$

References

[1] K.S. Yee, Numerical solution of boundary values problems involving Maxwell's equations in isotropic media, IEEE Trans. Antennas Propag. 14 (1966) 302–307.
[2] A. Taflove, S.C. Hagness, Computational Electrodynamics – The Finite Difference Time Domain Method, third ed., Artech House, Boston, 2005.
[3] W.L. Miranker, Difference schemes with best possible truncation error, Numer. Math. 17 (1971) 124–142.
[4] C.K.W. Tam, J.C. Webb, Dispersion-relation-preserving finite difference schemes for computational acoustics, J. Comput. Phys. 107 (1993) 262–281.
[5] J. Fang, Time Domain Computation of Maxwell's Equations, Ph.D. Dissertation, University of California at Berkeley, Berkeley, CA, 1989.
[6] E. Turkel, High order methods, in: A. Taflove (Ed.), Advances in Computational Electrodynamics – The Finite Difference Time Domain Method, Artech House, Norwood, 1998, pp. 63–110 (Chapter 2).
[7] K. Lan, Y. Liu, W. Lin, A higher order (2,4) scheme for reducing dispersion in FDTD algorithm, IEEE Trans. Electromagnet. Compat. 41 (1999) 160–165.
[8] E. Turkel, A. Yefet, On the construction of a high order difference scheme for complex domains in a Cartesian grid, Appl. Numer. Math. 33 (2000) 113.
[9] A. Yefet, E. Turkel, Fourth order compact implicit method for the Maxwell equations with discontinuous coefficients, Appl. Numer. Math. 33 (2000) 125.
[10] Z. Xie, C.H. Chan, B. Zhang, An explicit fourth order staggered finite difference time domain method for Maxwell's equations, J. Comput. Appl. Math. 147 (2002) 75–98.

[11] D.W. Zingg, H. Lomax, H. Jurgens, High-accuracy finite-difference schemes for linear wave propagation, SIAM J. Sci. Comput. 17 (1996) 328–346.
[12] J.L. Young, D. Gaitonde, J.J.S. Shang, Toward the construction of fourth-order difference scheme for transient EM wave simulation: staggered grid approach, IEEE Trans. Antennas Propag. 45 (1997) 1573–1580.
[13] P.G. Petropoulos, Phase error control for FD-TD methods of second and fourth order accuracy, IEEE Trans. Antennas Propag. 42 (6) (1994) 859–862.
[14] R.E. Mickens, Nonstandard Finite Difference Models of Differential Equations, Scientific World, Singapore, 1984.
[15] J.B. Cole, A high accuracy FDTD algorithm to solve microwave propagation and scattering problems on a coarse grid, IEEE Trans. Microwave Theory Tech. 43 (1995) 2053–2058.
[16] J.B. Cole, A high accuracy realization of the YEE algorithm using nonstandard finite differences, IEEE Trans. Microwave Theory Tech. 45 (1997) 991.
[17] J.B. Cole, High accuracy Yee algorithm based on nonstandard finite differences: new development and validations, IEEE Trans. Antennas Propag. 50 (2002) 1185.
[18] J.W. Nehrbass, J.O. Jevtić, R. Lee, Reducing the phase error for finite difference methods without increasing the order, IEEE Trans. Antennas Propag. 46 (1998) 1194.
[19] B. Yang, C.A. Balanis, An isotropy-improved nonstandard finite difference time domain method, IEEE Trans. Antennas Propag. 54 (7) (2006) 1935–1942.
[20] K.L. Shlager, J.B. Schneider, Comparison of the dispersion properties of higher order FDTD schemes and equivalent-sized MRTD schemes, IEEE Trans. Antennas Propag. 52 (4) (2004) 1095–1104.
[21] B. Yang, C.A. Balanis, Least square methods to optimize the coefficients of complex finite difference space stencils, IEEE Antennas Wireless Propag. Lett. 5 (2006) 450–453.
[22] H.E. Abd El-Raouf, E.A. El-Diwani, A.E.-H. Ammar, F. El-Hefnawi, A low-dispersion 3-D second-order in time fourth-order in space FDTD scheme (M3d24), IEEE Trans. Antennas Propag. 52 (7) (2004) 1638–1646.
[23] G. Sun, C.W. Trueman, Optimized finite difference time domain methods based on the (2, 4) stencil, IEEE Trans. Microw. Theory Tech. 53 (3) (2005) 832–842.
[24] G. Sun, C.W. Trueman, Suppression of numerical anisotropy and dispersion with optimized finite difference time domain methods, IEEE Trans. Antennas Propag. 53 (12) (2005) 4121–4128.
[25] S. Wang, F.L. Teixeira, A three dimensional angle optimized finite difference time domain algorithm, IEEE Trans. Microwave Theory Tech. 51 (2003) 811–817.
[26] S. Wang, F.L. Teixeira, Dispersion-relation-preserving FDTD algorithms for large-scale three-dimensional problems, IEEE Trans. Antennas Propag. 51 (2003) 1818–1828.
[27] S. Wang, F.L. Teixeira, A finite difference time domain algorithm optimized for arbitrary propagation angles, IEEE Trans. Antennas Propag. 51 (2003) 2456–2463.
[28] S. Wang, F.L. Teixeira, Grid dispersion error reduction for broadband FDTD electromagnetic simulations, IEEE Trans. Magn. 40 (2004) 1440–1446.
[29] T.T. Zygiridis, T.D. Tsiboukis, Low dispersion algorithms based on higher order (2,4) FDTD method, IEEE Trans. Microwave Theory Tech. 52 (2004) 1321–1327.
[30] T.T. Zygiridis, T.D. Tsiboukis, Higher order finite difference schemes with reduced dispersion errors for accurate time domain electromagnetic simulations, Int. J. Numer. Modell. 17 (2004) 461–486, doi:10:1002/jnm.551.
[31] T.T. Zygiridis, T.D. Tsiboukis, Design of optimized FDTD schemes for the accurate solution of electromagnetic problems, IEEE Trans. Magn. 42 (4) (2006) 811–814.
[32] N.V. Kantartzis, T.D. Tsiboukis, Higher Order FDTD Schemes for Waveguide and Antenna Structures, Morgan & Claypool Publishers, 2006.
[33] I.S. Koh, H. Kim, J.M. Lee, J.G. Yook, C.S. Pil, Novel explicit 2-D FDTD scheme with isotropic dispersion and enhanced stability, IEEE Trans. Antennas Propag. 54 (11) (2006) 3505–3510.
[34] G. Shen, A.C. Cangellaris, A new FDTD stencil for reduced numerical anisotropy in the computer modeling of wave phenomena, Int. J. RF Microw. Comput.-Aided Eng. (2007) 447–454.
[35] A.H. Panaretos, R.E. Diaz, A three-dimensional finite-difference time-domain scheme based on a transversely extended-curl operator, IEEE Trans. Microwave Theory Tech. 54 (12) (2006) 4237–4246.
[36] A.H. Panaretos, J.T. Aberle, R.E. Diaz, The effect of the 2-D Laplacian operator approximation on the performance of finite-difference time-domain schemes for Maxwells equations, J. Comput. Phys. 227 (1) (2007) 513–536.
[37] A.H. Panaretos, R.E. Diaz, A simple and accurate methodology to optimize parameter-dependent finite-difference time-domain schemes, IEEE Trans. Microwave Theory Tech. 56 (5) (2008) 1125–1136.
[38] B. Finkelstein, R. Kastner, Finite difference time domain dispersion reduction schemes, J. Comput. Phys. 221 (1) (2007) 422–438.
[39] B. Finkelstein, R. Kastner, FDTD Coefficient Modification Schemes of the Wave and Maxwell's Equations for Controlling Order of Accuracy and Dispersion Errors, Int. IEEE Symp. Antennas Propag., Honolulu, HI, USA, June 10–15, 2007.
[40] B. Finkelstein, R. Kastner, A comprehensive new methodology for formulating FDTD schemes with controlled order of accuracy and dispersion, IEEE Trans. Antennas Propag. 56 (11) (2008) 3516–3525.